ASSESSMENT OF POSITIONAL ACCURACY OF THE GLOBAL NAVIGATION SATELLITES SYSTEM (GNSS) STATIONS

BY

TATA HERBERT
(M. TECH/SV/08/0032)

OCTOBER, 2010

CHAPTER 1: INTRODUCTION

1.1 Background of Study

The Global Navigation Satellite System (GNSS) is a standard generic term used to describe a group of satellite based Navigation System that provides autonomous geo-spatial positioning with global coverage on or near the earth surface. At present, GNSS consist of the American controlled Global Positioning System (GPS), Russian controlled Global Orbiting Navigation Satellite System (GLONASS), the European Galileo and the China Compass. The Galileo and the Compass are still on test mode. As of today, GPS is the most widely utilized GNSS system, used in finding many applications within the areas of surveying, Navigation and recreation (Yaw and Gunter, 2006)

With respect to GNSS, countries can be categorized into three groups, those countries that own the satellite vehicles that generate the signals in space which includes the United states of America, with their Global Positioning System (GPS), Russia with their GLONSS, European union with their yet to be commissioned Galileo and China with their Compass which is still on test mode. The second group is made up of countries that have developed various augmentation system that improve the signals from the navigation satellite; these include The Japanese system is called MSAS which stands for MTSAT Satellite Augmentation System in which MTSAT stands for Multifunctional Transport Satellite System. India is developing GAGAN which stands for GPS Aided Geo Augmented Navigation. The third group includes countries that are yet to develop any sophisticated augmentation system; at best signals are improved by local area augmentation system. Countries in these groups are characterized by lack of GNSS infrastructures, expertise, and motivation to adopt this technology. (Yaw and Günter, 2006)

1.1.1 **Global Navigation Satellites System (GNSS) in African**

The introduction and implementation of satellite navigation technology to the development of the African continent is a right step in the right direction that needs to be pursued vigorously. In recognition of the strategic importance of satellite navigation, its potential in application and the need for the African states in joining the rest of the world to enjoy the benefits of the outer space; Organizations such as the International Civil Aviation Organization (ICAO), Africa and Indian ocean (AFI), the Agency for Air Navigation safety in Africa and Madagascar(ASECNA),the European Geostationary Navigation (EUROCONTROL) have been actively involved in inspirational collaboration to ensure the introduction and implementation of GNSS in Africa (Dodo and Kamarudin, 2007).

The African professionals such as the geodesist, until recently were skeptical with the use of GNSS especially in the field of surveying due to the perceived inaccuracies, probably due to the then selective availability and other errors that were associated with the GPS. With the modernization of GPS satellite, increased number of the satellite vehicles; tremendous improvement of the GNSS receiver technology; advances in the software development as well as the accuracies in satellite orbit broadcast, there is a very reliable level of accuracy as far as the requirement for most application in Africa are concerned (Yaw and Günter's, 2006)

1.2 Statement of Research problem

Many countries have set up their active GNSS stations and Real Time Kinematic (RTK) GPS Network Systems. Other countries are in the process of committing funds in order to set up their active GNSS stations. In some countries where these GNSS stations exist, they do not provide good coverage for network base RTK GPS. This is because the density of the network is not good enough; hence there are gaps in the converge. The strength of satellites signals received at each station varies from another. This is due to the availability of the satellites at the time the data are been downloaded. As a result of such, when a station is tracking data for it position, another station might not be receiving signals due to unavailability of the satellites.

Considering the service of these GNSS stations, some of the stations do not give complete 24hrs data but less than 24hrs data. In some cases, a whole 24hrs data is not provided. The quality of these data provided is also an area of concern, that is the percentage in terms of data quality, of some of the data is not of acceptance, yet the data are been downloaded and used for surveying and mapping. The reliability of these GNSS station lives much to be desired. Little or no much work has been done in order to ascertain the accuracies of these GNSS stations.

1.3 Motivation for the study

Due to the interest of so many countries in the used of GNSS data, as the world is becoming more global, these data are assessed through the internet for daily usage in surveying and mapping and also for Navigational purposes.

How reliable are these data that are obtained from the net? The passion to know the reliability and the accuracy of these data adopted as correct provide motivation for the research.

1.4 Aim and Objectives

The aim of this research is to assess the positional accuracies of the Global Navigation Satellite System (GNSS) Stations. These will be carried out using the following objectives:

(i) To evaluate the GNSS ground infrastructure.

(ii) Screening of the collected row RINEX data.

(iii) Processing of the GPS data

(i v) Analysis of the processed data

1.5 Research Scope

This will be based primarily on the ability of the collected GPS Receivers Independence Exchange (RINEX) data, Final orbit (ephemeris) data and the data processing technique to be employed so as to assess the accuracies of the positions of the GNSS stations. The area covered is limited to the Southern African Continuous Operating Reference Station (CORS) Network.

1.6 Overview of the study.

Chapter one gives the introduction of the study. This includes discussions on the general background, statement of problems, motivation, scope, aim and objectives of the study. An overview of the thesis for the study is also highlighted in this chapter.

In chapter two, the basic concept involved in GNSS positioning is discussed. The review of existing literatures on the problem identified in the study is carried out. The significance of the study is highlighted while the study area is also described.

Chapter three, deals with the methodology used for the research. This described the mode of data acquisition, types of data, instrumentation used and the quality of the data. Data processing strategy which involved various steps is also discussed in this chapter.

In chapter four, presentations and analysis of the results obtained using standard deviation are discussed. The analysis is divided into two parts; analysis base on coordinate difference and analysis base on residuals

Finally, in chapter five, conclusions on various findings are presented. Also, research contributions to knowledge and the recommendations based on the outcome of the study are highlighted.

CHAPTER 2: PRINCIPLE OF GNSS POSITIONING

2.1 Basic concept of GNSS positioning

GNSS stands for Global Navigation Satellite Systems. The Global Position System (GPS) is the best known of these satellite navigation systems. Global Navigation Satellite System (GNSS) is the standard generic term for satellite navigation systems that provide autonomous geo-spatial positioning with global coverage. A GNSS allows small electronic receivers to determine their location (longitude, latitude, and height) to within a few metres using the signals as transmitted by the GNSS satellites. In the same process the receivers also calculate the precise time of the signal reception and as such GNSS receivers can be used as highly accurate clocks.

2.2 Evaluation of Global Navigation Satellite System (GNSS)

The Global Navigation Satellite System (GNSS) is a space-based radio positioning system that include one or more satellite constellations, augmented as necessary to support the intended operation, and that provides 24-hours three dimensional position, velocity and time information to suitably equipped users any where on, or near the surface of the earth.

GNSS is a generic term covering a number of existing and planned constellations of satellites together with supporting infrastructure system, used for determining positions across the globe. The core element of GNSS includes: the Global positioning system (GPS), the Global Orbiting Navigation Satellite System (GLONASS), and the planned Galileo system (Dodo and Kamarudin, 2007).

2.2.1 Global Positioning System (GPS)

In 1973 a project group was formed with representatives of the U.S. armed forces and the Defense Mapping Agency to develop a new navigation and positioning system. This new satellite positioning system, which would replace the old DOPPLER- or TRANSIT-navigation system, became known as the NAVSTAR GPS. Where NAVSTAR stands for “NAVigation by Satellite Timing And Ranging”, and GPS for “Global Positioning System”. The system was put into operation by the U.S. Department of Defense for the military force to accurately determine their positions, velocity and time in a common reference system, any where on or near the Earth on a continuous basis. Originally, GPS was developed to meet military requirement, which was quickly adopted by the civilian world with some restrictions. The Usage of GPS has enormously increased and has included more applications with the elimination of SA (selective availability). GPS consist of three major segments; namely a spaces segment; a control segment and a user segment (Ndukwe, 2001).

2.2.1.1 Space Segment

The space segment (SS) is composed of the orbiting GPS satellites or Space Vehicles (SV) in GPS parlance. The GPS design originally called for 24 SVs, eight each in three circular orbital planes, but this was modified to six planes with four satellites each. The orbital planes are centered on the Earth, not rotating with respect to the distant stars. The six planes have approximately 55° inclination (tilt relative to Earth's equator) and are separated by 60° right ascension of the ascending node (angle along the equator from a reference point to the orbit's intersection) The orbits are arranged so that at least six satellites are always within line of sight from almost everywhere on Earth's surface.

The constellation, Orbiting at an altitude of approximately 20,200 kilometers above the surface of the earth, with orbital period of approximately 11 hours 58 minutes. The constellation provides global coverage with four to eight satellite simultaneously observed about 15 ^{0} elevation. The orbital configuration is illustrated in Figure 2.1

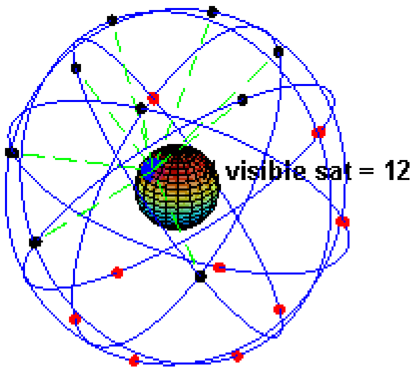

Figure 2.1 GPS orbital configuration

The GPS satellites provide a platform for radio transmitters, computers, and various equipments, used for positioning, timing, Radio Frequency (RF) transmission and for a series of other military projects. The satellites are equipped with solar panels for power supply, reaction wheels for attitude control, and a propulsion system for orbit adjustments. Each satellite has highly accurate timing standards derived from rubidium and cesium clocks. The electronic equipment of the satellites allows the user to measure a pseudrange to the satellite, and each satellite to broadcast a message, which allows the user to recognize the satellite and to determine its position in space for arbitrary epochs. Each satellite transmits on two modulated signal (Agnew, and Larson, 2007).

2.2.1.2 Control Segment for GPS

The operational control system (OCS) consists of a master control station, monitor station, and ground control station. The master control station control station is located at Schriever Air Force Base in Colorado Springs. The master control station collects the tracking data from five monitoring stations and calculates the satellite orbit and clock parameters. These results are then passed to one of the three ground station for eventual upload to the satellites. The five monitor station are equipped with precise cesium time standards and receivers that continuously measure range data to determine the broadcast ephemeris as well as model the satellite clocks. The ground stations mainly consist of antennas that receive the satellites ephemeris and clock information and upload them to each GPS satellite.

The control station is also responsible for establishing GPS Time, which is defined as the number of seconds elapsed from Saturday midnight of the present week. GPS time is realized by an atomic time scale, which is related to UTC (Universal Time Coordinate). GPS time is synchronized with UTC at the microsecond level, within an integer number of seconds. GPS satellites transmit clock corrections, which model the deviation of the clocks with respect to GPS time. The deviation is less than 1 ms and corrections are accurate to within a few nanoseconds (Lachapelle, 2001).

2.2.1.3 User Segment

The User Segment is composed of hundreds of thousands of U.S. and allied military users of the secure GPS Precise Positioning Service, and tens of millions of civil, commercial and scientific users of the Standard Positioning Service. In general, GPS receivers are composed of an antenna, tuned to the frequencies transmitted by the satellites, receiver-processors, and a highly-stable clock (often a crystal oscillator). They may also include a display for providing location and speed information to the user. A receiver is often described by its number of channels: this signifies how many satellites it can monitor simultaneously.

The primary focus in the early years of GPS developers was on navigation for civilian use, but the surveying community quickly adopted the system for high-accuracy positioning. The use of GPS in the civilian community is expanding rapidly due to the decrease in receiver costs. The user segment consists of receiver's technologies for computing local position/navigation solutions, in addition to the receiver clock offset. The GPS satellites positions are computed in the earth-centered Earth-fixed WGS-84 reference system, such that a user's position is referenced to the WGS-84 ellipsoid. GPS receivers come in a variety of formats, from devices integrated into cars, phones, watches and also Geodetic GPS Receivers to dedicated devices such as those shown in figure 2.2 from manufacturers of Trimble, Garmin and Leica (Kaplan, 1996).

Figure 2.2 Dual Frequency Trimble GPS receivers

2.2.1.4 The Global Positioning System Signals

All signals transmitted by the satellite are derived from the fundamental frequency (f_0) of the satellite oscillator. The two carrier frequencies, f_1 and f_2 (the corresponding wavelengths are 19 and 24 cm), are modulated with the codes and the navigation message to transmit information such as the readings of the satellite clocks, the orbital parameters, etc. The C/A-code (Coarse-Acquisition, Clear-Access, or Civil-Access) is modulated on the f_1 carrier only. The P-code (Precise or Protected) is modulated on both carriers. There are two limitations for civilian users, namely Selected Availability and Anti-Spoofing, briefly referred to as SA and AS, respectively. Both deteriorate the achievable accuracy for civilian users significantly. Selective Availability (SA), the denial of full accuracy, is accomplished by "manipulating" navigation message orbit data (epsilon) and/or the satellite clock frequency (dither). So far, only the satellite clock frequency has been manipulated. With this dithering process the GPS satellite clocks are artificially degraded by adding a signal with an unknown frequency and amplitude to the know clock behavior. This is done to degrade the performance of GPS for the “normal” users. Both, the frequency and amplitude of the added signal, change rapidly over time. The amplitude of this “clock dithering” is of the order of 0.3 microseconds (which corresponds to roughly 100 meters) and the frequency is of the order of only a few minutes. This SA clock dithering limits the accuracy of real time position estimates to 25 meters RMS (Moore, 1997). The Selective Availability was removed at midnight GMT on May 1, 2000 (www.ngs.naa.gov)

Anti-spoofing (AS) is a protection against “fake” transmissions by encrypting the P-code to form the Y-code. This ensures that the GPS signals cannot be disturbed (spoofed) by a GPS-like transmitter on the Earth. The anti-spoofing procedure converts the P-code to the Y-code which is only usable when a secret conversion algorithm is available to the receiver. The Y-code is the “modulo two sum” of the P-code and the encryption code, also referred to as the W-code. Only selected (military) users have access to the conversion algorithm. The effect of AS is that civilian users have only access to the C/A-code and therefore only to one single frequency. This disables the possibility to eliminate ionospheric refraction using observations on two different frequencies. This further limits the accuracy for the civilian users. For real time non-differential applications, the SA effect limits the accuracy to about 100 meters. At this accuracy level the effect of AS is negligible because both, the effects of a more precise code and the ionosphere, are negligible compared to the 100 meter level SA effect. For real time differential GPS AS is the accuracy limiting factor. In differential applications, the

SA effect cancels out almost completely. The accuracy is in this case limited by the degraded accuracy of the code and by ionospheric refraction (PosiTim, 2009)

2.2.1.5 GPS Constellation

The presently available full constellation guarantees simultaneous observations of at least four to eight GPS satellites from (almost) every point on the surface of the earth at (almost) every time of the day. This is accomplished by 24 satellites (21 plus 3 active spares) located in six orbital planes in almost circular orbits with an altitude of about 20 200 km above the surface of the Earth (Onyeka, 2007). The orbital plane is inclined by 55 degrees with respect to the equator. The sidereal revolution period of the GPS satellites is 11 hours 58 minutes (approximately half a sidereal day). Consequently, the same satellite configuration is repeated 4 minutes earlier every day for one and the same location.

2.2.2 Global Orbiting Navigation Satellite System (GLONASS)

Development of GLONASS began in 1976, with a goal of global coverage. GLONASS was developed to provide real-time position, accuracy and velocity determination, initially for use by the Soviet military in navigating and ballistic missile targeting.

The Global Orbiting Navigation Satellite System (GLONASS), it is a Russian system, similar to GPS. The latest launch of 3 satellites was successful in December 2004 (PosiTim, 2007). This brought the total number of GLONASS satellites in orbit to 14. Eleven satellites are now in operation, including the first GLONASS-M satellite.

2.2.2.1 GLONASS Constellation

A fully operational GLONASS constellation consists of 24 satellites, with 21 used for transmitting signals and three for in-orbit spares, deployed in three orbital planes. The three orbital planes' ascending nodes are separated by 120° with each plane containing eight equally spaced satellites. The orbits are roughly circular, with an inclination of about 64.8°, and orbit the Earth at an altitude of 19,100 km, which yields an orbital period of approximately 11 hours, 15 minutes. The planes themselves have a latitude displacement of 15°, which results in the satellites crossing the equator one at a time, instead of three at once. The overall arrangement is such that, if the constellation is fully populated, a minimum of 5 satellites are in view from any given point at any given time. This guarantees for continuous and global navigation for users world-wide. Each satellite is identified by a "slot" number, which defines the corresponding orbital plane and the location within the plane; numbers 1-8 are in plane one, 9-16 are in plane two, and 17-24 are in plane three (Onyeka, 2007).

A characteristic of the GLONASS constellation is that any given satellite only passes over the exact same spot on the Earth every eighth sidereal day. However, as each orbit plane contains eight satellites, a satellite will pass the same place every sidereal day. For comparison, each GPS satellite passes over the same spot once every sidereal day. So opposed to the GPS the ground-track of the GLONASS satellites do not repeat after one day. This avoids the resonance effects which makes station keeping of GPS satellites difficult and expensive (Onyeka, 2007).

2.2.3 Galileo

Galileo will be Europe's own global navigation satellite system, providing a highly accurate, guaranteed global positioning service under civilian control. It will be inter-operable with GPS and GLONASS, the two other global satellite navigation systems. A user will be able to take a position with the same receiver from any of the satellites in any combination. By offering dual frequencies as standard, however, Galileo will deliver real-time positioning accuracy down to the metre range, which is unprecedented for a publicly available system. It will guarantee availability of the service under all but the most extreme circumstances and will inform users within seconds of a failure of any satellite.

The Galileo programme is Europe's initiative to develop a civil global navigation satellite system that provides highly accurate and reliable positioning, navigation and timing services. Galileo will be compatible and interoperable with GPS and GLONASS, offering multiple civil frequencies. The fully developed Galileo system will consist of 30 satellites and the associated ground infrastructure (Dodo and Ono, 2007).

2.2.3.1 Galileo Constellation

The fully deployed Galileo system will consist out of 30 satellites, 27 operational satellites and 3 active in orbit spares. The Galileo satellites will be positioned in three circular Medium Earth Orbital (MEO) planes with an altitude of 23222 km above the Earth. This means the Galileo satellites are above the GPS and GLONASS satellites. The so called "repeat cycle" for the Galileo satellite orbits is 10 days. The orbital revolution period, being 14 hours and 7 minutes.

The inclination of the orbital planes will be 56 degrees with reference to the equatorial plane. In full orbit constellation (FOC) the Galileo navigation signals will provide good coverage even at latitudes up to 75 degrees north, which corresponds to the North Cape, and beyond. The large number of satellites together with the optimization of the constellation, and the availability of three active spare satellites, will ensure that the loss of one satellite does not affect the end users of the system (Dodo and Ono, 2007).

2.2.4 COMPASS/ Beidou

The COMPASS system (also known as Beidou-2) is a project by China to develop an independent satellite navigation system. The current Beidou-1 system (made up of 4 satellites) is experimental and has limited coverage and application. However, with the COMPASS system, China plans to develop a truly global satellite navigation system consisting of 35 satellites.

The new system will be a constellation of 35 satellites, which include 5 geostationary orbit (GEO) satellites and 30 medium Earth orbit (MEO) satellites that will offer complete coverage of the globe. COMPASS will offer 10 services. Five free open services, and five restricted authorized services. These services will be centered at eight different carrier frequencies. The free service will have a 10 meter location-tracking accuracy, will synchronize clocks with an accuracy of 50 ns, and measure speeds within 0.2 m/s. The authorized (or licensed) service will be more accurate than the free service, can be used for communication, and will supply information about the system status to the users (PosiTim, 2007).

2.3 Global Positioning System (GPS) Surveying

2.3.1 Static Surveying

The static observation procedure is the most commonly used GPS observation technique due to its reliability and ease of data collection. The results generated from static observations are the most robust of the GPS positioning solutions due to the increased length in observation period. All control surveys over reference/rover separations of several kilometres are performed using static surveying techniques. The Static procedure requires satellite measurements to be acquired simultaneously at multiple sites by stationary receivers.

Static surveys are performed by setting receivers on stable platforms, usually a tripod or survey pillar and leaving them to record measurements at predetermined intervals for a period of time. Observations are usually collected at a rate of one epoch every 5, 10, 15 or 30 seconds. The rate of collection is not of prime importance in static work and measurements should be acquired at rates which are related to the amount of available data storage space. More importantly, data needs to be collected for a sufficient time period to enable the integer cycle ambiguities to be determined. In addition, the effects of multipath and random measurement error can be reduced by observing for long period. There are no hard rules for determining how long data should be collected. The time required to achieve a suitable accuracy is a function of the number of visible satellites, baseline length, multipath conditions, atmospheric conditions and satellite geometry. Using past experience and knowledge, the surveyor may choose an observation period that he or she feels is sufficient to resolve ambiguities and obtain an accurate position (Onyeka, 2007).

To make full use of the acquired measurements, static surveys should be post-processed. This requires the storage of the observables to be merged in the processing software at a later time. This implies that results are not available in the field, as well as, implying that the time period required to obtain a required accuracy is a calculated guess. Experience under similar survey conditions generally defines the observation period, however, for accurate results, observation periods of less than 30 minutes should not be used for lines greater than five kilometres in length. Observation periods will also need to be longer if single frequency 'receivers are used as wide-lane and narrow-lane combinations will not be able to be formed. It should be noted that the longer the observation session, the more accurate the calculated position would be. If post-processing reveals that results are unsatisfactory, the baseline will need to be observed again. It is; therefore, wise to use caution when estimating observation periods as an additional five or ten minutes per point may be sufficient to prevent further observation (Onyeka, 2007).

2.3.2 Rapid Static Surveying

The rapid static surveying technique was developed in an attempt to improve the efficiency of the static survey procedure. Users should note that the observation procedures for rapid static surveying are the same as those for static surveying. The only difference is the length of the occupation period which is less than that required for static surveys. In order to perform surveys with maximum efficiency, a dual frequency receiver which is capable of pseudorange and carrier phase measurements on both carrier frequencies is required. This enables the wide-lane and narrow-lane phase combinations to be used to aid in the estimation of the ambiguities. The use of the pseudorange measurements (after they have been smoothed) also assists in the rapid determination of the ambiguities, therefore, receivers capable of code measurements in the presence of anti-spoofing are desirable.

As the occupation period of rapid static surveys is shorter than that of static surveys, it can often be extremely difficult to manage the movement of receivers in sessions. Therefore, rover receivers generally occupy points as efficiently as possible. Occupation times as short as ten minutes are often sufficient to resolve the integer ambiguities over short baselines when at least six satellites are tracked. This results in a series of radiation type vectors from the reference station. To provide some redundancy, a second reference station may be used. This provides two vectors to each point. It should be noted that this method of data collection is unsuitable for detecting erroneous vectors if the rover station is the source of error. An example of such an error is incorrect entry of the antenna height. A second occupation of each station, ideally using a different reference receiver, is preferable; however, this reduces survey efficiency. Surveyors must use their professional discretion in a manner in which rapid static surveys are conducted (Onyeka, 2007).

The rapid static survey procedure is most efficient when dual frequency receivers are used and baselines are kept below five kilometres. If the points of interest are free of overhead obstructions and six or more sufficient satellites are observed, surveys can be performed in a matter of minutes (Onyeka, 2007).

2.3.3 Stop And Go Kinematic Surveying

The kinematic survey procedure was developed in the mid 1980's as an attempt to improve the productivity of surveying with GPS receivers. In applications where a large number of points spaced are less than few kilometres apart and need to be coordinated, these static procedures are inefficient and are, generally, not cost effective. The kinematic survey technique is ideally suited to such applications where points are closely spaced and easily accessed.

Once the carrier phase integer cycle ambiguities have been determined, they do not change value if continuous tracking of the satellites is maintained, i.e. there are no cycle slips. The kinematic survey procedure is based on this characteristic of carrier phase positioning. A Short initialisation procedure is performed with the primary aim of determining the integer ambiguity values. Once this initialisation is completed, the rover receiver occupies points of interest for a short period, generally, less than one minute. As the ambiguities do not change when satellites are continuously tracked, centimetre level accuracy can be obtained with a brief stationary occupation. Once a point has been occupied, the rover moves to the next point of interest where it acquires another minute of data. During the period in which the receiver is being transported between the two sites, satellite tracking must be maintained. This technique of continually moving, then stopping briefly, is termed Stop and Go Kinematic Surveying.

The Stop and Go Kinematic Surveying procedure is performed to coordinate the position of stationary marks. The receiver must still continuously track satellites while in motion to preserve the integer ambiguity estimates. However, the position of the receiver while moving is not of interest. If cycle slips are experienced while moving, the integer ambiguity term for the interrupted satellite must be calculated again. If at least four satellites are still being tracked, this can be performed automatically by the processing software without user intervention. This is possible as the receiver can calculate its position using the remaining satellites. This position is then held fixed (constrained) and the unknown integer ambiguity estimated. This technique is termed the known baseline initialisation and is performed frequently when cycle slips are present. If the cycle slips cause the number of satellites to drop below four, the survey must be reinitialised to determine the integer ambiguities as their values will have changed. There are four ambiguity initialisation techniques which can be used at any time throughout a kinematic survey. Some of the techniques are more reliable than others and more strongly recommended (Ndukwe, 2001).

2.3.4 Continuous Kinematic Surveying

The continuous kinematic survey technique is identical to the stop and go procedure, except the position of the receiver while it is in motion is now of interest. As long as the satellites are tracked without interruption, the position of the antenna can be estimated at each measurement epoch. The epoch rate must be set carefully to ensure that position estimates are computed at a desirable frequency. Surveyors should build redundancy into kinematic surveys by occupying marks on multiple occasions, or in the continuous kinematic case, re-traverse the same route. One feature of continuous kinematic surveys that must be considered is whether the height of the receiver is of interest while the receiver is in motion. If this is the case, then the height of the antenna above the ground must be kept uniform. This can be accomplished using a range of devices, many of which are best developed by the surveyor for a specific use (Ndukwe, 2001).

2.3.5 Real Time kinematic (RTK) Surveying

The satellite carrier phase measurements collected at both reference and rover receivers can be stored using a number of different media, and then combined in a computer for post-processing. The restriction of this approach is that the results of the survey are not known until after the survey has been completed. Real time processing techniques utilise a data link, usually in the form of a radio, to transfer corrections acquired at the reference receiver (set up on a survey mark) to the rover receiver. The microprocessor in the rover receiver then combines the reference and rover information and computes the rover coordinates as the survey is being performed: this is called real time kinematic surveying. The corrections broadcast are the difference between the known coordinates of the survey mark and the calculated coordinates of the survey mark by the reference receiver.

This capability enables surveyors to check coordinates in the field, ensure surveys are being performed successfully and facilitate establishment of features at predetermined locations (setting out). lf the GPS equipment facilitates all four initialisation methods, then surveyors can simply occupy marks and wait until the receiver display indicates that the ambiguities have been resolved by the on the fly method. The antenna swap essentially becomes obsolete as occupation of previous marks (known baseline), static survey and the on the fly technique can be used in combination to perform surveys more efficiently. The major advantage of this field procedure is that users are aware of the status of the survey as it is being performed. Therefore, surveys can be performed to maximum efficiency as the minimum amount of data required to resolve the integer ambiguities can be determined (Ezeigbo, 1998).

2.3.6 On The Fly

On the fly resolution, computes the integer ambiguities while the receiver is in motion. To perform this efficiently, a minimum of five satellites are required, however, six or seven satellites are preferred. In addition, on the fly techniques should not be attempted with single-frequency receivers as the process is extremely inefficient. The advantage of this technique for surveyors is that previous marks do not need to be located frequently for initialisation purposes. An example of the flexibility of the on the fly initialisation procedure is where a surveyor collects observations of points, then passes under a bridge. With the on the fly technique, the surveyor can continue moving to the next feature of interest. While the surveyor is moving, the satellites will be re-acquired and the on the fly resolution scheme will automatically begin to resolve the ambiguities.

In general, the ambiguities are safely resolved in less than five minutes. In most instances, two minutes of tracking six or seven satellites is sufficient. Once initialised, the survey can proceed as normal. Users should note that, if there are only four satellites being tracked, the on the fly technique cannot operate. In addition, if five satellites are observed, or the satellite geometry is poor, initialisation times may exceed ten or fifteen minutes.

2.4 GPS Errors

2.4.1 Carrier Phase-Based Differential GPS Error Sources

Differencing GPS measurements eliminates both receiver and satellite clock errors. These are, therefore, not discussed any further herein. The remaining GPS errors are classified into two groups: (i) spatially uncorrelated errors; and (ii) spatially correlated errors. The spatially uncorrelated errors - namely, receiver noise and multipath - depend on receiver types, antenna types and antenna environment. They are not reduced by operation in differential GPS (DGPS) mode. Employing a high quality receiver and antenna and antenna location in an open sky-tracking location with minimal multipath effects contribute to increasing data quality and reducing uncorrelated errors. The spatially correlated errors, including satellite orbital error, tropospheric and ionospheric errors -are a function of inter-antenna distance and atmospheric conditions. They, therefore, can be reduced in DGPS operation. As each error source has its own characteristics, they are described in the following sections (IGS 2004).

2.4.2 Satellite Orbital Error

In order to estimate the unknown positioning states using GPS measurements, one must know the satellite positions, which are reported in an ephemeris. The satellite positions are predicted using a set of Keplerian orbit, perturbation, and satellite clock parameters (Kaplan et al 1996). Satellite orbital errors are caused by inaccurate estimations of satellite positions reported in the ephemeris. The most obvious way to reduce the satellite orbital error is by using a precise ephemeris, which allows the user to calculate the satellite positions within accuracy of better than 5 cm (IGS 2004). The precise ephemeris is provided by various GPS agencies such as the International GPS Service (IGS), the US National Geodetic Survey (NGS) and the Geodetic Survey Division, Natural Resources Canada (GSD/NRCan). However, the precise ephemeris is available only in post-mission. For example, users must wait 12 days for a final precise ephemeris, 17 hours for a rapid ephemeris and 3 hours for an ultra-rapid ephemeris. For most real times or near real-time applications, the broadcast ephemeris transmitted along with satellite navigation messages is used. The satellite positions calculated from the broadcast ephemeris have an RMS error of approximately 2 m (IGS 2004).

A satellite's orbital error is spatially correlated and is reduced using DGPS. According to Wells et al (1986), the relationship between a satellite orbital error and the resulting baseline error in DGPS is

$$\frac{\Delta d}{d} = \frac{\Delta \rho}{\rho} \tag{2.1}$$

Where Δd is the total error in length of the baseline d (m), $\Delta\rho$ is the total error in the coordinates of a satellite position (m), and ρ is the mean distance from the stations to the satellite (m). Based on Equation (2.1), the baseline error caused by a satellite position error of 2 m is less than 1 cm for baseline lengths of up to 100 km, assuming an average satellite receiver distance of 20200 km. This effect is negligible for DGPS, typically at the centimetre level of accuracy.

2.4.3 Atmospheric Erros

2.4.3.1 Ionospheric Error

The ionosphere is a layer at approximately 50 km to 2000 km above the earth's surface and is a very important source of errors in GPS measurements. It is formed by the ionization of the neutral atmosphere by solar ultraviolet radiation (UV) and X-ray radiation coming from the corona of the Sun at low and middle altitudes and by energetic particles at high altitude (Skone 1998). The ionosphere itself is approximately plasma, meaning that it is electrically neutral as a whole with equal numbers of electrons and ions. Within this sphere, the electrons gather around ions with a certain plasma frequency and spin along the magnetic field, resulting in collisions between electrons and ions (Skone 1998). GPS signals can travel through the ionosphere but may be attenuated, depending on the signal frequency, electron collisions and the electron density along the traveling path. The first-order slant ionospheric carrier phase error in units of metres, I , is (Leva *et al* 1996)

$$I = \left[1 - \frac{R_e \cos\alpha}{R_e + h_1}\right]^{\frac{1}{2}} \frac{40.3VTEC}{f^2} \qquad (2.2)$$

where R_e is the radius of the earth, α is satellite elevation, h_I is the height of the ionosphere above the earth's surface, f is the carrier frequency of the GPS signal, and VTEC stands for Vertical Total Electron Content in units of electrons/m^2. VTEC represents the electron density in a vertical column along the GPS signal trajectory, a quantity that varies with location and level of ionospheric activity. The electron number per unit of volume, moreover, changes with altitude:

increasing from altitude of 50 km, reaching its peak of 1012 electrons/m^3 at an altitude of 300 to 350 km, and then decreasing significantly at higher altitudes. The ionosphere is also divided into different regions, namely D, E, F1, F2 and H based on their altitudes and characteristics (Klobuchar, 1996). The D region (at altitude of 50 km -90 km) and the E region (at altitude of 90 km – 140 km) place negligible effects on GPS measurements (Klobuchar 1996). The F1 and F2 regions at altitude of 140 km – 210 km and 210 km – 1000 km, respectively, place the most significant impact on GPS measurements. The H region at altitude of larger than 1000 km and its impact on GPS measurements can be significant under storm conditions (Klobuchar 1996).

The magnitude of the ionospheric error varies depending on the process of ionization, which depends mainly on the nature of solar activities. It is, therefore, different from day to night and from one season to another. Diurnally, the ionospheric error usually reaches its first peak at 14:00 local time, its secondary peak at 22:00 local time and drops to the 15 minimum before sunrise. This diurnal effect is the result of a variation in the electron number created and depleted through processes of ionization and recombination caused by the diurnal period of the Sun (Skone 2003). Seasonally, the ionospheric error is larger in winter (October to March for Calgary) versus summer (April to September for Calgary) due to the slower recombination process of free electrons caused by cold molecular nitrogen N_2 (Skone 2003). Another characteristic of the ionosphere is the equatorial anomaly. This is caused by the neutral wind motions pushing electrons to the two sides of the magnetic equator (± 10° magnetic latitude) resulting in a higher electron density in these regions (Skone 2003). The very complex interaction between the solar, wind and the magnetosphere, which is formed outside the ionosphere due to the magnetic character of the earth itself, results in some ionospheric phenomena including sudden ionospheric disturbance (SID), polar cap absorption, aurora oval, magnetic storm and ionospheric storm (Skone 1998, Liu 2004), SID phenomena are caused by solar flares, which comprise transient brightening in a small active area on the solar surface leading to a sudden increase in TEC in the D, E and F regions of the ionosphere. The flares typically last from only a few minutes to several hours (Liu 2004). Large travelling solar flares produce many highly energetic protons, leading to intense ionization in some areas. This phenomenon is called polar cap absorption and is ordinarily observed at high latitudes of more than 75o geomagnetic latitude (Skone 1998). This event usually lasts for long periods of time (a few days) but, fortunately, is rather rare. The auroral oval is a region of the ionosphere characterized by a high geomagnetic latitude of 65-67o night side and of 75-85o dayside (Skone 1998). Enhanced conductivity and energetic electrons are formed in the auroral regions, especially under storms. The phenomenon is caused mostly by the solar wind but its complexity is not fully explained in existing literature (Skone 1998). A magnetic storm is a global-scale event caused by a large sudden change in solar wind pressure on the magnetopause, resulting in disturbances of the geomagnetic field. An ionospheric storm is characterized by irregularities in electron density in the F region of the ionosphere. Ionospheric impact on GNSS signals is very significant under storm conditions due to highly localized electron density and scintillations. In addition to large measurement errors, loss of phase lock and cycle slips are the other most common impacts caused by a highly active ionosphere. Very fortunately, the ionospheric effect is dispersive to GPS frequencies and therefore can be modeled or eliminated using dual frequency combinations. However, under extreme conditions, losing lock or cycle slips remain a problem even with the use of dual-frequency ionospheric-free combinations.

There are many techniques available to model the ionospheric error to a certain level of accuracy. One such model, the Klobuchar model, is based on the satellite broadcast ephemeris and is capable of modeling only 50% of the ionospheric error (Klobuchar, 1996). Two-dimensional (2D) modeling techniques approximate the ionospheric error based on dual frequency measurements from a network of GPS stations, giving real-time or near real-time ionospheric corrections to users. These techniques consider the ionosphere as one unique layer at a fixed height above the earth (usually from 50 km to 500 km). There are two types of 2D models: function-based and grid-based. The function-based technique fits the zenith ionospheric delay observed at reference stations into a surface, which is usually described by a function of pierce points of the GPS signals on the ionosphere layer. The grid-based algorithm is more widely used than function-based one. Using this technique, the GPS network geographical region is covered by a grid with precisely known coordinates and a certain degree of density depending on the size of the GPS network. The zenith ionospheric delay at each GPS reference station is estimated based on the GPS dual frequency observations. These estimations are then interpolated to the position of each grid point. The ionospheric delay at a given rover's position located inside the coverage area is estimated by interpolating the estimated delays at the four surrounding grid points. For a DGPS user who has access to the dual frequency L1 and L2 GPS measurements, the most common method of significantly reducing the ionospheric effect on DGPS positioning is by using the GPS dual frequency measurements. The following equation represents the relationship between ionospheric error on GPS L1 and L2 measurements

$$L_2 = \left(\frac{\lambda_2}{\lambda_1}\right) L_1 \qquad (2.3)$$

An ionospheric-free (IF) observation combination should be used when the inter-antenna distance is long or under unsettled ionospheric conditions. The ionospheric error can also be stochastically modeled using dual frequency observables.

2.4.3.2 Tropospheric Error

The troposphere is neutral atmosphere, which means that it does not contain free electrons, and occupies the region from approximately 0 to 43 km above the earth's surface. The tropospheric error does not depend on solar activities. It is not GPS frequency-dependent and therefore cannot be eliminated by using a dual-frequency combination. The troposphere places two major delay effects on GPS measurements due to its dry component and its wet component (Skone 2003). The dry delay contributes approximately 90% of the total delay; however, the dry component is a function of local temperature and pressure, both of which vary relatively slowly. The dry delay is thus easily modeled. The wet delay is caused by a high concentration of water vapour at heights of between 0 and 15 km above the earth's surface. It constitutes only 10% of the total delay. However, this component is hard to predict and model due to the nature of the surface humidity variation. Being dependent on the humidity along the signal path, the troposphere also has a seasonal effect on GPS observations. In Calgary, it is generally more humid during summer than during winter, meaning that the tropospheric error on GPS measurements (mainly its wet component) is generally larger in summer than in winter (de Jong *et al* 2002). In winter, especially when it is very cold (-20 to -30^{o}C), the tropospheric error could drop to a negligible value (de Jong et al, 2002). However, a large amount of wet snow or rain can change the situation, due to the increase in water vapour, increasing the tropospheric error considerably for high precision GPS techniques. Generally, tropospheric effects on GPS signals reach 2 to 5 metres for a satellite at zenith and up to approximately 25 metres for a satellite at low elevation, for example, in the range of 5o (Skone, 2003).

In order to obtain the slant tropospheric effects, the effect at zenith is firstly modeled. A mapping function is then used to map the zenith delay to a certain angle of observation. The tropospheric model used in this thesis is the Goad – Goodman model. The total tropospheric error at zenith, D^{z}_{trop} (h $)_{user}$, is the sum of the dry error caused by the dry component, D^{z}_{d} , and the wet error caused by the wet component, D^{z}_{w} , and can be calculated as follows (Skone 2003)

$$D^{z}_{trop}(h_{user}) = D^{z}_{d} + D^{z}_{w} \qquad (2.4)$$

with the dry and wet components expressed as

$$D^{z}_{d} = \tfrac{10^{-6}}{5} N_{do}(h_{d} - h_{user})\, for h_{user} \leq h_{d} = 43km \qquad (2.5)$$

$$D_w^z = \tfrac{10^{-6}}{5} N_{wo}(h_w - h_{user})\, for h_{user} \le h_w = 12km \qquad (2.6)$$

$$N_{do} = 77.604\left(\tfrac{p_d}{T}\right)\left(\frac{1}{1+p_d\left[57.97e^8\left(1+\frac{0.52}{T}\right)-9.4661e^{-4}\,{}^{Tc}\!/_{T^2}\right]}\right) \qquad (2.\ 7)$$

$$N_{wo} = (\tfrac{e}{T}\left(1+1650\tfrac{e}{T^3}\left[1-0.01317T_c + 1.75_e{}^{-4}T_c^2 + 1.44e^{-6}T_c^3\right]\right)\left(64.79+\tfrac{377.600}{T}\right) \qquad (28)$$

Where h_{user} is the height of the rover, h_w is the maximum height of the wet component, h_d is the maximum height of the dry components, N_{w0} represents the wet refractivity and N_{d0} stands for the dry refractivity at the earth's surface. As shown in equation (2.7), the refractivity components are a function of temperature T (T_c is temperature in degrees Celsius and T_K is temperature in degrees Kelvin), dry air pressure P_d in millibars and partial pressure of the water vapour e in millibars. The partial pressure of the water vapour is estimated as a function of relative humidity R_h and temperature T. A mapping function is used to map the zenith value to the slant value, as follows

$$\mu = \frac{1}{\sin(\alpha)} \qquad (2.8)$$

Where α is the satellite elevation of the measurement. This is the simplest form of mapping functions. However, it is adequate in this case due to the use of high elevation cut off angle, which is 15 degrees.

2.4.4 Receiver Error

2.4.4.1 Multipath and Noise

Multipath, interference and noise have very short spatial correlation characteristics (Parkinson & Enge 1996). This means that the effect of these error sources obtained at a reference station can be very different from those obtained at a rover station when using the DGPS technique. Multipath occurs when the antenna receives both reflected and direct signals. Multipath depends highly on the reflector's properties, the antenna reflector distance, the antenna gain pattern and the type of correlator used in a receiver (Ray 2000). The resulting impact on GPS carrier phase measurements is less than one quarter of the carrier wavelength (Ray 2000). Multipath in static observations is typically non-Gaussian and follows a sinusoidal trend. In kinematic applications, multipath has a more random behaviour due to dynamic disturbances of the receiver. The effect of multipath is very short when correlated over the distance and therefore cannot be reduced using DGPS.

Receiver noise is due mainly to thermal noise, dynamic stress and oscillator stability in the tracking loop of the receiver (Lachapelle 2003). It has a very small effect (in the order of mm in magnitude) on carrier phase positioning. Differential GPS, in fact, approximately doubles the receiver noise, as compared to single point GPS. Similarly, using multiple reference stations result in more noise in the filter than using one reference station.

2.5 Accuracy Enhancement

Global Navigation Satellite System, accuracy can be classified in four stages; Augmentation, Precise monitoring, Time keeping and carrier phase tracking.

2.5.1 Augmentation

Integrating external information into the calculation process can materially improve accuracy. Such augmentation systems are generally named or described based on how the information arrives. Some systems transmit additional error information (such as clock drift, ephemera, or ionospheric delay), others characterize prior errors, while a third group provides additional navigational or vehicle information (Parkison, 1996).

2.5.2 Precise monitoring

Accuracy can be improved through precise monitoring and measurement of existing GPS signals in additional or alternate ways.

After the Selective Availability (SA) was turn off by the U.S government, The largest remaining error is usually the unpredictable delay through the ionosphere. The spacecraft broadcast ionospheric model parameters, but errors remain. This is one reason GPS spacecraft transmit on at least two frequencies, L1 and L2. Ionospheric delay is a well-defined function of frequency and the total electron content (TEC) along the path, so measuring the arrival time difference between the frequencies determines TEC and thus the precise ionospheric delay at each frequency. Military receivers can decode the P(Y)-code transmitted on both L1 and L2. Without decryption keys, it is still possible to use a codeless technique to compare the P(Y) codes on L1 and L2 to gain much of the same error information. However, this technique is slow, so it is currently available only on specialized surveying equipment. In the future, additional civilian codes are expected to be transmitted on the L2 and L5 frequencies. Then all users will be able to perform dual-frequency measurements and directly compute ionospheric delay errors.

A second form of precise monitoring is called Carrier-Phase Enhancement (CPGPS). This corrects the error that arises because the pulse transition of the PRN is not instantaneous, and thus the correlation (satellite-receiver sequence matching) operation is imperfect. CPGPS utilizes the L1 carrier wave, which has a period of $\frac{1\sec}{1575.42*10^{6}} = 0.63475 nano\sec ond \approx 1 nano\sec ond$ which is about one-thousandth of the C/A Gold code bit period of $\frac{1\sec}{1575.42*10^{3}} = 977.5 nano\sec ond \approx 100 nano\sec ond$, to act as an additional clock signal and resolve the uncertainty. The phase difference error in the normal GPS amounts to 2–3 metres (6.6–9.8 ft) of ambiguity. CPGPS working to within 1% of perfect transition reduces this error to 3 centimeters (1.2 in) of ambiguity. By eliminating this error source, CPGPS coupled with DGPS normally realizes between 20–30 centimetres (7.9–12 in) of absolute accuracy (Parkison, 1996).

Relative Kinematic Positioning (RKP) is a third alternative for a precise GPS-based positioning system. In this approach, determination of range signal can be resolved to a precision of less than 10 centimeters (3.9 in). This is done by resolving the number of cycles in which the signal is transmitted and received by the receiver. This can be accomplished by using a combination of differential GPS (DGPS) correction data, transmitting GPS signal phase information and ambiguity resolution techniques via statistical tests—possibly with processing in real-time (real-time kinematic positioning, RTK) (Parkinson,1996)

2.5.3 **Timekeeping**

While most clocks are synchronized to Coordinated Universal Time (UTC), the atomic clocks on the satellites are set to GPS time. The difference is that GPS time is not corrected to match the rotation of the Earth, so it does not contain leap seconds or other corrections that are periodically added to UTC. GPS time was set to match Coordinated Universal Time (UTC) in 1980, but has since diverged. The lack of corrections means that GPS time remains at a constant offset with International Atomic Time (TAI) (TAI - GPS = 19 seconds). Periodic corrections are performed on the on-board clocks to correct relativistic effects and keep them synchronized with ground clocks (Parkinson, 1996).

The GPS navigation message includes the difference between GPS time and UTC, which as of 2009 is 15 seconds due to the leap second added to UTC December 31, 2008. Receivers subtract this offset from GPS time to calculate UTC and specific timezone values. New GPS units may not show the correct UTC time until after receiving the UTC offset message. The GPS-UTC offset field can accommodate 255 leap seconds (eight bits) which, given the current rate of change of the Earth's rotation (with one leap second introduced approximately every 18 months), should be sufficient to last until approximately the year 2300 (Parkison,1996).

As opposed to the year, month, and day format of the Gregorian calendar, the GPS date is expressed as a week number and a seconds-into-week number. The week number is transmitted as a ten-bit field in the C/A and P(Y) navigation messages, and so it becomes zero again every 1,024 weeks (19.6 years). GPS week zero started at 00:00:00 UTC (00:00:19 TAI) on January 6, 1980, and the week number became zero again for the first time at 23:59:47 UTC on August 21, 1999 (00:00:19 TAI on August 22, 1999). To determine the current Gregorian date, a GPS receiver must be provided with the approximate date (to within 3,584 days) to correctly translate the GPS date signal. To address this concern the modernized

GPS navigation message uses a 13-bit field, which only repeats every 8,192 weeks (157 years), thus lasting until the year 2137 (157 years after GPS week zero) (Parkison,1996).

2.5.4 Carrier phase tracking

Another method that is used in surveying applications is carrier phase tracking. The period of the carrier frequency times the speed of light gives the wavelength, which is about 0.19 meters for the L1 carrier. Accuracy within 1% of wavelength in detecting the leading edge reduces this component of pseudorange error to as little as 2 millimeters. This compares to 3 meters for the C/A code and 0.3 meters for the P code. However, 2 millimeter accuracy requires measuring the total phase—the number of waves times the wavelength plus the fractional wavelength, which requires specially equipped receivers. This method has many surveying applications.

Triple differencing followed by numerical root finding, and a mathematical technique called least squares can estimate the position of one receiver given the position of another. First, compute the difference between satellites, then between receivers, and finally between epochs. The satellite carrier total phase can be measured with ambiguity as to the number of cycles. Let $\phi(r_i, s_j, t_k)$denote the phase of the carrier of satellite j measured by receiver i at time t_k. This notation shows the meaning of the subscripts i, j, and k. The receiver (r), satellite (s), and time (t) come in alphabetical order as arguments of $\phi$and to balance readability and conciseness, let $\phi_{i,j,k} = \phi(r_i, s_j, t_k)$be a concise abbreviation. Also we define three functions, :$\Delta^r, \Delta^s, \Delta^t$, which return differences between receivers, satellites, and time points, respectively. Each function has variables with three subscripts as its arguments. These three functions are defined below. If $\alpha_{i,j,k}$is a function of the three integer arguments, i, j, and k then it is a valid argument for the functions, :$\Delta^r, \Delta^s, \Delta^t$, with the values defined as

$$\Delta^r(\alpha i, j, k) = \alpha i + 1, j, k - \alpha i, j, k, \qquad (2.9)$$

$$\Delta^s(\alpha i, j, k) = \alpha i + 1, j, k - \alpha i, j, k, \text{and} \qquad (2.10)$$

$$\Delta^t(\alpha i, j, k) = \alpha i + 1, j, k - \alpha i, j, k, \qquad (2.11)$$

Also if $\alpha_{i,j,k}$ and $\beta_{l,m,n}$are valid arguments for the three functions and a and b are constants then $(a\ \alpha_{i,j,k} + b\ \beta_{l,m,n})$is a valid argument with values defined as

$$\Delta^t(\alpha\alpha i, j, k + b\beta l, m, n) = \alpha\Delta^r(\alpha i, j, k) + b\Delta^r(\beta l, m, n), \qquad (2.12)$$

$$\Delta^s(\alpha\alpha i, j, k + b\beta l, m, n) = \alpha\Delta^s(\alpha i, j, k) + b\Delta^s(\beta l, m, n), \text{and} \qquad (2.13)$$

$$\Delta^t(\alpha\alpha i, j, k + b\beta l, m, n) = \alpha\Delta^t(\alpha i, j, k) + b\Delta^t(\beta l, m, n), \qquad (2.14$$

Receiver clock errors can be approximately eliminated by differencing the phases measured from satellite 1 with that from satellite 2 at the same epoch. This difference is designated as $\Delta^s(\phi_{1,1,1}) = \phi_{1,2,1} - \phi_{1,1,1}$

Double differencing computes the difference of receiver 1's satellite difference from that of receiver 2. This approximately eliminates satellite clock errors. This double difference is:

$$(\Delta^r(\Delta^s(\phi 1,1,1)) = \Delta^r(\phi 1,2,1 - \phi 1,1,1) = \Delta^r(\phi 1,2,1) - \Delta^r(\phi 1,1,1) = (\phi 2,2,1 - \phi 1,2,1) \qquad (2.15)$$

Triple differencing subtracts the receiver difference from time 1 from that of time 2. This eliminates the ambiguity associated with the integral number of wave lengths in carrier phase provided this ambiguity does not change with time. Thus the triple difference result eliminates practically all clock bias errors and the integer ambiguity. Atmospheric delay and satellite ephemeris errors have been significantly reduced. This triple difference is: $\Delta^t \left(\Delta^r \left(\Delta^s \left(\phi 1,1,1\right)\right)\right)$

Triple difference results can be used to estimate unknown variables. For example if the position of receiver 1 is known but the position of receiver 2 unknown, it may be possible to estimate the position of receiver 2 using numerical root finding and least squares. Triple difference results for three independent time pairs quite possibly will be sufficient to solve for receiver 2's three position components. This may require the use of a numerical procedure. An approximation of receiver 2's position is required to use such a numerical method. This initial value can probably be provided from the navigation message and the intersection of sphere surfaces. Such a reasonable estimate can be key to successful multidimensional root finding. Iterating from three time pairs and a fairly good initial value produces one observed triple difference result for receiver 2's position. Processing additional time pairs can improve accuracy, over determining the answer with multiple solutions. Least squares can estimate an over determined system. Least squares determines the position of receiver 2 which best fits the observed triple difference results for receiver 2 positions under the criterion of minimizing the sum of the squares (Parkison,1996).

2.2 Literature review

Global Navigation Satellite system (GNSS) have evolved from an early period of limited programs such as the American global positioning System (GPS) and the Russian Global Navigatsionnya Sputnikovaya System (GLONASS) to a period where a number of system and their augmentations where developed. The idea was to build more GNSS station which will increase accuracy to the users of GNSS and at the same time, to increase the integrity, availability and continuity of the system (Dodo and Kamarudin, 2007).

The history of GNSS is largely that of the US Global Positioning System (GPS), which is now over 30 years old. During this time there have been other satellite navigation and positioning systems, including the Transit Doppler system, which preceded GPS itself, but is no longer operational. Others include the Russian Global Satellite Navigation System (GLONASS), Beidou of China, the regional Wide Area Augmentation Systems WAAS in the United States, EGNOS in Europe and MSAS in Japan. The European Global Satellite Navigation System Galileo is still to be deployed and declared operational sometime between 2008 and 2010 (Nottingham Scientific, 2005).

In june 1992, the International GPS Service (IGS), renamed International GNSS Service in 2005, produce and make available uninterrupted time series of its products. Some of the product includes GPS observations from the IGS Global Network, GPS orbits (broadcast, ultra rapid, rapid and final orbit), Earth orientation parameters (components Easting and Northing of polar motion, length of day) with daily time resolution, satellite and receiver clock. The study stated that in each day, different latencies and accuracies were taken. On weekly batches, the coordinate and velocities were taken, so that can be use for further analysis of accuracy and positioning (Beutler et al, 2008**).**

Introducing Global Navigation Satellite System into Africa means creating opportunities for regional and international technological advances, resulting in a wide range of economic and social benefit, when it purpose of providing positioning accuracy is being achieved (Dodo and Kamarudin, 2007**).**

In a study "An Evaluation of the Global Navigation Satellite System (GNSS) Ground infrastructure in Africa" conducted by Dodo and Ono (2007) revealed that the Global Navigation satellite System (GNSS) is one of the space technology that has the ability of adding value with serious contribution in the areas of positioning and location. The essential systems of GNSS are the GPS, GLONASS and the incoming Galileo. Despite the fact that, the systems are globally accepted; they still have some technical limitation in the areas of integrity, accuracy, availability and continuity. The study further shows that issues of system integrity, accuracy, availability and continuity are not adequately address, so as to meet the standard required.

Global Positioning System (GPS) technology has become an essential tool in the Earth observation field for geo- referencing, classification and accuracy assessment activities. The GPS was originally developed to be employed primarily in the open area; some of the GPS users nowadays operate GPS receivers in less favourable conditions. An investigation was carried out on the impact of varying types and degrees on GPS data collection, accuracy and position. It is discovered that the occurrence of canopy overhead may degrade the positional precision and accuracy, due to poor signal reception cause by the canopy. The result of the study shows that for proper reception of the signal in order to achieve the accuracy, position and the precision required, then GPS observation should be carried out in open areas (Sigrist et al, 1999**).**

Farah et al (2008) stated that all African countries have started embracing the idea of using the applications of GNSS technologies particularly Global Positioning system (GPS) in the various geo information applications, services and its products. The study, further explains that GPS technology can be use in the implementation of the African references frame (AFREF). The successful implementation of the AFREF depends on the application of Global Navigation Satellite System (GNSS). It is expected of the GNSS system to be consistent and to provide the required positional accuracy, in order to achieve the aim of embracing it usage and application; most of the African stations are currently distributed in the Eastern, Southern Africa and part of Western African coastal region.

The IGS network stations in Africa have increased slowly during the last five years. It was predicted that in the near future, several additional stations will be installed by HartRAO in collaboration with international partners. These IGS station will form an important node for Africa. Little or nothing has been done in the area of their accuracy (Combrinck, 2002**).**

In a study conducted by Walperdorf et al, (2007) assess the availability and quality of data from the International GNSS Service (IGS) Global Positioning System (GPS) network in Africa, especially for retrieving Zenith Tropospheric Delay (ZTD). The result shows that the major sources of error for the GPS data analysis evaluation in Africa that affect the accuracy of GPS are the Ionosphere and the troposphere. The accuracy was assessed through position dispersion between individual solutions and the most recent version of the IGS combined solution with the International Terrestrial Reference Frame. After the assessment the positioning performance of the IGS analysis were consistent with accuracy as requested for meteorological applications.

GPS Network is restricted by the effect of some atmospheric refraction on the GPS signals. Two main components cause this atmospheric refraction leading to the restriction on GPS Network. There are the ionospheric and tropospheric refraction. The troposphere bias is the major sources of error in the GPS Network, which limit the fully functionality of the GPS positioning. The data obtained were used to reduce the tropospheric effect. The data used for the study were in observational format. The international GNSS service (IGS) station which is located in Singapore was used as the reference station, which the RINEX data observed were taken of in daily basis (Dodo and Kamarudin, 2007).

In a study conducted by Mohd and Kamarudin (2007) stated that, when the satellite signals of the Global positioning system (GPS) passed through the earth's neutral atmosphere, the radio signals are been affected by variability of refractive index which cause delay in the arrival of the GPS signals. With out proper compensation, the delay affects the accuracy of GPS derived position, which is the concern for high accuracy application. Due to these tropospheric delays, RINEX data of myRTKnet from five GPS reference station in johor were integrated with GPS and local meteorological observations, looking at the discrepancies of the

GPS measurement. The result of the study state that in neglecting the use of a standard tropospheric model, it will lead to variation of accuracy and positioning.

Dodo et al (2008), stated that one of the major problems currently facing satellite based positioning is the atmospheric error/delay of the GPS signal, caused by the troposphere. The study was conducted by using four campaigns with each campaign for three days. Real time kinematics GPS network (RTKnet) references station were used. The result reveals that there is inconsistency in the Troposphere delay variations.

In a study conducted by Chai and Tseng, (1999) stated that, the effect of the atmosphere has become one of the major limiting factors affecting accuracy for GPS positioning. Using improved instrument, a high level of positioning precision will be achieved when the observed data are been processed. Atmospheric effect on GPS signals consists of the Ionospheric and tropospheric delays. The Ionospheric delay can be eliminated by the application of the double Ionospheric free combination. The tropospheric delay can only be reduced by the use of tropospheric models. This study was carried out with the aim of investigating the effect of the tropospheric modeling by applying standards atmospheric models for GPS positioning. It was done by tracking a number of GPS station in order to test the effect of the tropospheric delay affecting the network signals thereby bring about limitation in accuracy and position of GPS.

The global positioning System (GPS) has been widely used for precise positioning and accuracy applications throughout the world. With that in mine, there are still some limiting factors that reduce the performances of satellite based positioning and it accuracy. With GPS ranges measurement made on two frequencies, it allows for direct correction of the Ionospheric bias for single point positioning application. This reveals that precise positioning and accuracy could be improved with accurate Ionospheric models, but unfortunately the models are no specifically designed for précised positioning application. In order to test the ability of existing Ionospheric models to derive the relative change in the ionosphere, a permanent network of continuously tracking from GPS station was required. The result stated that, although the models are Global in nature, they are constrained to the general nature of input coefficients and are therefore unable to adequately estimate ionosphere behaviors, which in return affect if positioning and accuracy (Wyllie and Zhang 2003).

Roberts, (2004) conducted a research in which GNSS CORS Network in Australia was used. The study reveal that, the standard mode of high accuracy positioning, required the use of one Global positioning system (GPS) receiver to be located at a reference station with known coordinates, while the second "user" receiver simultaneously tracks the same satellite signals. The study went further to state that many application of Global Navigation satellite system GNSS technology, such as surveying mapping and precise Navigation, requires real- time positioning accuracies.

In order to support these application, many countries are establishing dense CORS network with there station well positioned. The projects investigate the enhancements of network so as to maintain similar levels of positioning and accuracy as dense CORS networks. The result of the study revealed that, with a better understanding and modeling of atmospheric condition, which are currently the major limitation in high accuracy technique, of GPS positioning are required so as to achieved the goals of there accuracy and positioning

2.7 Significance of the Research

From the review of previous works, it is discovered that most of the work deals mostly on GPS errors and on the augmentation of the GNSS stations, without considering weather these station that are been establish still maintain there positions. This study is to assess the positions of these GNSS stations to see how accurate and reliable there are when been used for surveying and mapping. Similarly, the study will contribute knowledge on how satellite planning is important to satellite surveying and also serve as an eye opener giving confidence to those downloading GNSS data from the internet and to the countries that are into the augmentation of these GNSS stations.

2.8 Study Area

The use of GNSS data is widely acceptable within the African community as a solution for high accuracy in position determination. This allows the assessment of accuracy in position on the GNSS stations, so as to enhance positioning accuracies of these stations. The study is the Southern African Continuous Operating Reference Stations (CORS) Network. Reason been that, the stations contribute data to the IGS and these stations are the realization of the ITRF 2000, as such, they can be used as reference station by any country.

Southern Africa is the southernmost region of the Africa continent, variably defined by geography or geopolitics. The terrain of Southern African varied, ranging from forest and grasslands to deserts. The region has both low – lying coastal areas and mountains. It is located between latitude 00^0 55’N to 34^0 18’S and longitude 9^0 54’E to 30^0 55’E (Encarta Encyclopedia, 2009). Figure 2.3 shows the network which consist of the following GNSS stations; Simon’stown GNSS Station with ID number simo, Rechardsbay GNSS Station with ID number rbay, the Pretoria GNSS Station with ID number harb, Uganda GNSS Station with ID number mbar and Lebreville GNSS Station with ID number nklg.

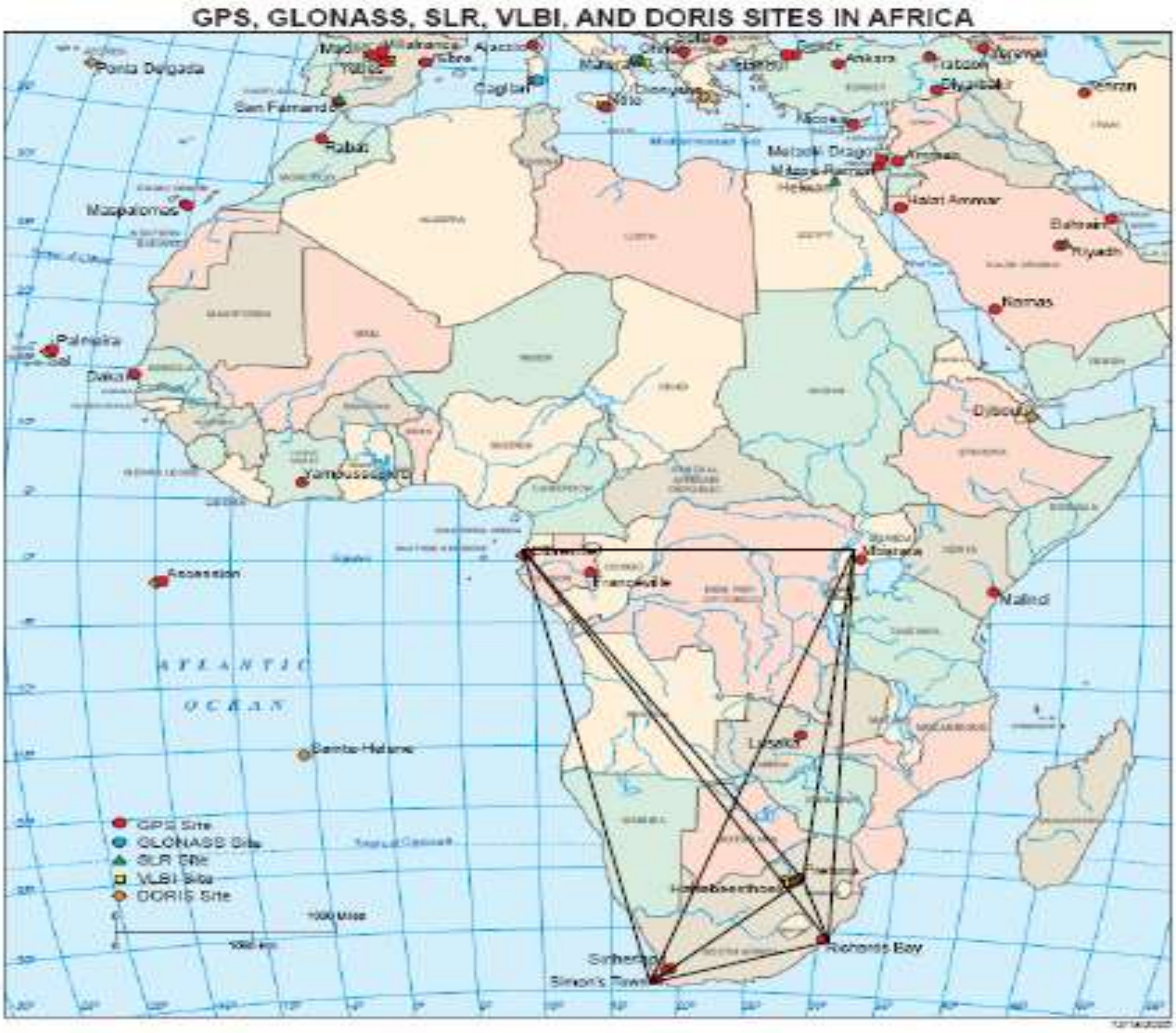

Figure 2.3 showing the location of GNSS Stations in the study area

2.8.1 Description of the GNSS Stations in the Study Area

2.8.1.1 Harttebeesthoek GNSS Station (harb)

Hartebeesthoek is a GNSS Station located at Pretoria in the Republic of South Africa. The site has an identification name known as HARB. The site was installed on the 9th August 2000. The first logging of the site took place on the 12th November 2000 and was prepared for used on the 15th October 2008. Three types of instrument are mounted on the site namely; Doppler Orbitography Radiopositioning Integrated Satellite (DORIS), Very Long Baseline Interferometry (VLBI) and the combination of (GPS/ GLONASS/ DORIS/ SLR/ VLBI/). Three types of GNSS Receivers are mounted on this site namely; ROUGE SNR – 8000, TRIBLE 4000SSI and, ASHTECH U2 – 12. In tracking of signal three antennas are mounted, there are AOAD / M_T, TRM29659.00 and A20.

Fig 2.4 showing the harb site

2.8.1.2 Richardsbay GNSS Station (rbay)

Richardsbay is a GNSS Station located at Kwa – Zulu Natal State in South Africa. The site has an identification name known as RBAY. The site was installed on the 10th October 2000. The first logging of the site took place on the 2nd June 2008 and was prepared for used on the 3rd July 2008. The combination of (GPS/

GLONASS/ DORIS/ SLR/ VLBI/), are the type of instrument mounted on the site, with it GNSS Receivers as; ROUGE SNR – 8000 and A20. In tracking of signal two antennas are mounted, there are AOAD / M_T, and A20.

Fig 2.5 shows the rbay site

2.8.1.3 Simonstown GNSS Station (simo)

Simonstown is a GNSS Station located at Western Cape State in South Africa. The site has an identification name known as SIMO. The site was installed on the 26th July 2007. The first logging of the site was on the 21st April 2008 and was prepared for used on the 8th July 2008. The combination of (GPS/ GLONASS/ DORIS/ SLR/ VLBI/), are the type of instrument mounted on the site, with it GNSS Receivers name as; ROUGE SNR – 8000. In tracking of signal two antennas are mounted, there are; AOAD / M_T, and A20.

Fig 2.6 showing simo site

2.8.1.4 N’koltang GNSS Station (nklg)

N’koltang is a GNSS Station located at Libreville city of Gabon in the premise of Ariane tracking Station. The site has an identification name known as NKLG. The site was installed on the 10th February 2000. The first logging of the site took place on the 24th of January 2008 and was prepared for used on the 10th December 2008. Two type of instrument are mounted on the site namely; DORIS and the combination of (GPS/ GLONASS/ DORIS/ SLR/ VLBI), with it GNSS Receivers as; TRIBLE 4000SSI and A20. TRM29659.00 and A20 are the type of antenna mounted on that site.

Fig 2.7 showing nklg site

2.8.1.5 Mbarara GNSS Station (mbar)

Mbarara is a GNSS Station located at Kyhi Forest Resave State in Uganda. The site has an identification name known as MBAR. The site was installed on the 20th march 2000. The first logging of the site took place on the 30th June 2008 and was prepared for used on the 3rd July 2008. The combination of (GPS/ GLONASS/ DORIS/ SLR/ VLBI), are the type of instrument mounted on the site, with it GNSS Receivers names as; ASHTECH Z – XIIS and A20. In tracking of signal two antennas are mounted, there are ASH 701945B_M SCIS and A20.

Fig 2.8 showing mbar

CHAPTER 3: METHODOLOGY

3.1 General Statement

In this study, the converted RINEX data into an observational data were used for processing. Thereafter, a statistical method of standard deviation was used in assessing the accuracy of the positions of the GNSS stations.

3.2 Data Acquisitions

In order to have an optimal result for this research, the GPS RINEX data and the Final Satellite Orbital data (Ephemeris) data were downloaded from the internet. The data downloaded were for Day of the Year (DoY) 12, 44, and 68 in the year 2007, 186 and 195 in 2008 and 001,002 in 2009. The selected days were as the result of the availability and quality of the data. These data were downloading from two website namely; The International GNSS Service website (IGS) and Scrip Orbit and Permanent Array Center website (SOPAC). The following data were used for the research work namely:

(a) **GPS RINEX data (Raw data)**

RINEX format is a globally accepted format that has been designed to facilitate post – processing GPS data collected using receivers developed by different manufacturers. The RINEX format specifies three files, an observational file which contains the measured pseudoranges and carrier phase, an ephemeris file which contains the satellite orbit parameters, and an optional meteorological file which contains station surface meteorological readings.

These GPS RINEX data (Raw data) were downloaded from the SOPAC website. The downloaded data were in compact format which were later converted into an observational format using a Hatanaka conversion program. These data were for (DoY) 12, 44, and 68 in the 2007, 186 and 195 in 2008 and 001,002 in 2009 for the following station; harb ,mbar, nklg, rbay and simo.

(b) Final Satellite Orbital data (Ephemeris data)

The GPS Final Orbits data were downloaded from the IGS website. These data were for day 5 in week 1409, day 2 in week 1414 and day 5 in week 1417 for the year 2007, day 0 in week 1488 and day 5 in week 1486 for the year 2008, day 4 in week 1512 and day 5 in 1512 for the year 2009. Figure 3.1 below shows data acquisition design.

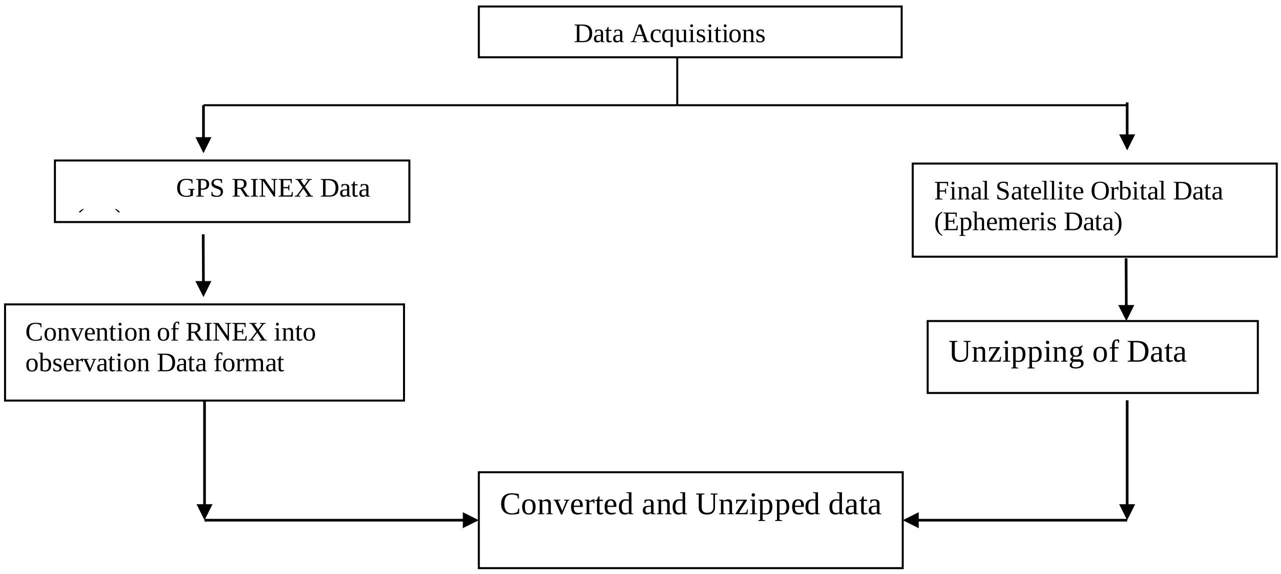

Figure 3.1 data acquisition design

3.3 Data quality

Quality of data used for any experiment can be determined by the validity and reliability of such data based on the assumption that the observers of such data are trust worthy and experienced. The validity of the data is measured by the precision of the instrument used while the reliability of data is determined by the accuracy of such data.

The raw RINEX data and ephemeris data were used for the purpose of this project. The data were downloaded from two websites which are globally acceptable bearing in mine that, geodetic GPS receivers were used for tracking the data which has been found to be of very accuracy (IGS, 2004).

3.4 Types of Instrument used

The following instruments were used for data processing:

(a) Hardware

(i) Dell laptop computer with 2GB RAM and a Hard disk of 160GB with a processor speed of 2GHz

(ii) HP DeskJet F4200 Series printer

(b) Software

(i) Trimble Total Control Software

(ii) Hatanaka conversion program

(iii) WinZip version 145 Software

3.5 Satellite Planning

Planning is essential to satellite surveying just as reconnaissance survey is important to land surveying. Planning is of great importance to monitor a survey campaign. It answers questions on the best time of observation with respect to satellite visibility, satellite elevation, Satellite dilution of precision (DOP).

In fig 3.1 Shows a visibility graph for all satellite available and the periods in which these satellite are visible. From the graph it indicates that from the hour of

21:00hrs to 24:00hrs no satellites were available. From 24:00hrs to 12:00hrs few satellite were available and from 12:00hrs to 24:00hrs most satellites were available. Indication the best time to carry out satellite observation.

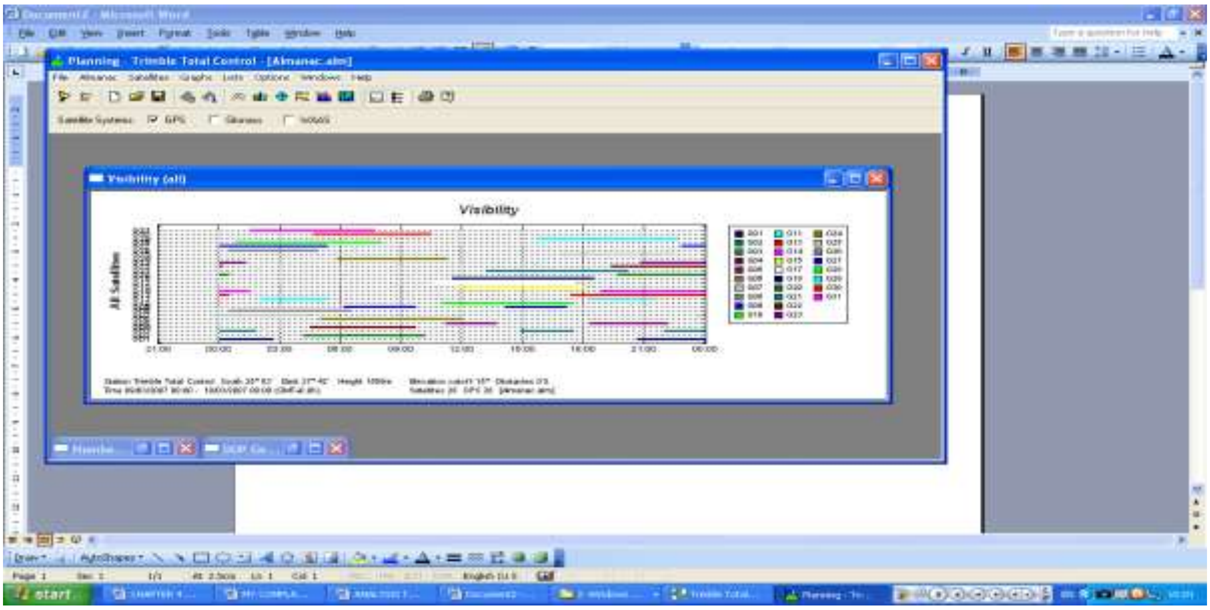

Fig 3.2 showing a graph of satellite visibility

3.6 Data Processing Strategy

This section described the step by step method on how the data obtained were processed. Two type of data set were used; the raw RINEX data and the ephemeris data. The raw RINEX data was in compact format were converted into an observational format before processing. The ephemeris data were in zip format and were unzipped before processing. The data set used include; day of the Year (DoY) 12, 44, 68 in 2007; 186 and 195 in 2008 and 001, 002 in 2009. The first step was the importing of the observational data into the Trimble Total Control Software (TTC) followed by the ephemeris data. The processing parameters set before processing are listed below. The start time and the end time set before the processing depends on the satellites are availability. Data logged from 02:26:31am to 22:59:30pm were used in the processing. In all sessions of processing, station harb was held fixed as the control station in the baseline estimations of the network in which all other station were referenced too. Processing was done on static mode at 30 seconds. The required solution type (frequency) that is the Ionospheric free error (Lc) was set at 5km with the GPS cutoff angel at 15^0. For an effective result, the precise obit type was used. Goad and Goadman (fixed values) Troposheric models were used by default for static method which described the atmospheric conditions in the troposphere, to improve the processing result. The processing of the baseline is done automatically after selecting the option to process the baselines. This was achieved in the following steps;

(i) Create a project

(ii) Import the Converted and unzipped Data

(iii) Setting of the processing parameters which will include:-

  (a) Cut off angel of 15^0

  (b) Orbit type – Precise Orbit

  (c) Troposheric models – Goad and Goadman

  (d) Residuals data

  (e) Processing range.

  (f) Preference

  (g) Processing mode

  (h) frequency

(iv) Baseline Processing

(v) Perform Network Adjustment (Constrained)

(vi) Displaying of the final Adjusted positions

(vii) Data Analysis

(viii) Positions Dispersion Analysis. Figure 3.3 shows processing design.

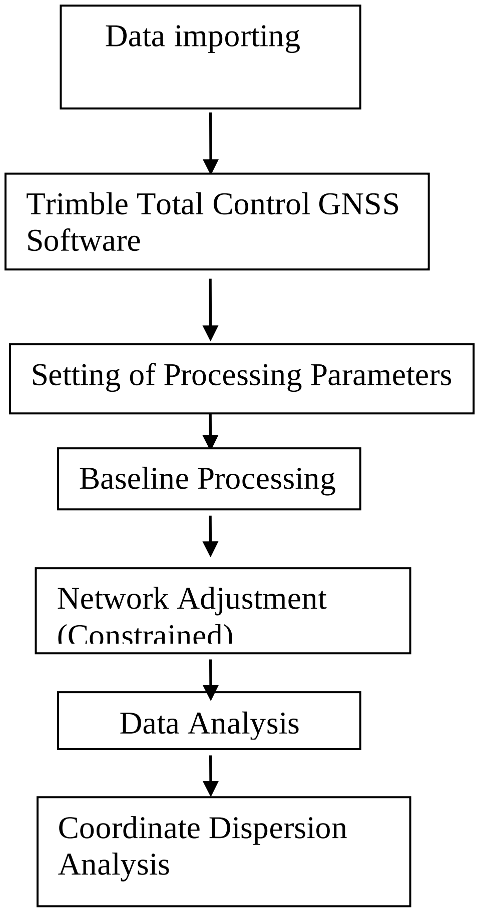

Figure 3.2 shows processing design

CHAPTER 4: PRESENTATION AND ANALYSIS OF RESULTS

4.1 Presentation of Result

Table 4.1 below shows the approximate coordinate of the stations, which were established initially using precise GPS surveying method and later were linked to International Terrestrial References Frame (ITRF) 2000. The sites information or these stations were obtained from the SOPAC website. GPS surveying baseline is the position of one receiver relative to another. When the data from two receivers are combine, the result is a baseline comprising a three dimensional vector between the two points. Table 4.1 shows approximate positions of the station in ITRF 2000.

Station ID	Northings(m)	Eastings (m)	Height (m)
harb	5084658	2670325	-2768481
mbar	5482951.388	3260442.643	-66519.8489
nklg	6287385.872	1071574.413	39132.764
rbay	4739765.812	2970758.377	-3054077.646
simo	5010435.805	1670594.692	-3563732.513

Table 4.1 Approximate positions of the Stations in ITRF 2000

In table 4.2 below, are the baseline length of the stations with referenced from control point to other stations. From table 4.2 below, the baseline length from harb - nklg is the longest having about 3447.500km, while harb - rbay have the shortest baseline length of 535.236km. The longer the baseline the more errors are likely to occur and the shorter the baseline the better the result. The baseline from harb to rbay will have a better result than the baseline from harb to nklg (Tajul, 2006). Table 4.2 shows the baseline length from harb

From Station ID	To station ID	Baseline length (km)
harb	**mbar**	2794.185
harb	**nklg**	3447.500
harb	**rbay**	535.236
harb	**simo**	1275.607

Table 4.2 baseline length from harb

Figure 4.1 below, shows a sample of a processed baseline for DoY 68 in the year 2007. The processed baseline shows two different colours, the yellow color and green color. The yellow colour indicate that, the baseline was successfully processed, ambiguities are not fixed, and the standard deviation less than the default standard deviation provided by the Trimble Total Control (TTC) software. The Ionosphere free carrier phase combination (LC) was used in processing of the baseline because the baselines were longer than the default length (5km). In processing of the baseline, the primary L band (L1) carrier was used by GPS satellite to transmit satellite data. In other words, it is carrier frequencies (signal), in which the GPS satellites transmit information. Its frequency is 1575.42 MHZ. It is modulated by C/A code, P code and a navigation message, the secondary L band (L2) carrier used by GPS satellite to transmit satellite data. In other words, it is carrier frequencies (signal), in which the GPS satellites transmit information. It frequency is 1227.60 MHZ. It is modulated by, P code and a navigation message and Lc is an ionosphere free carrier phase combination. It is the combination of both the L1 and the L2 which can process baseline longer than the default length given. The green colour indicates that the baseline was successfully processed, and the ambiguities are fixed;

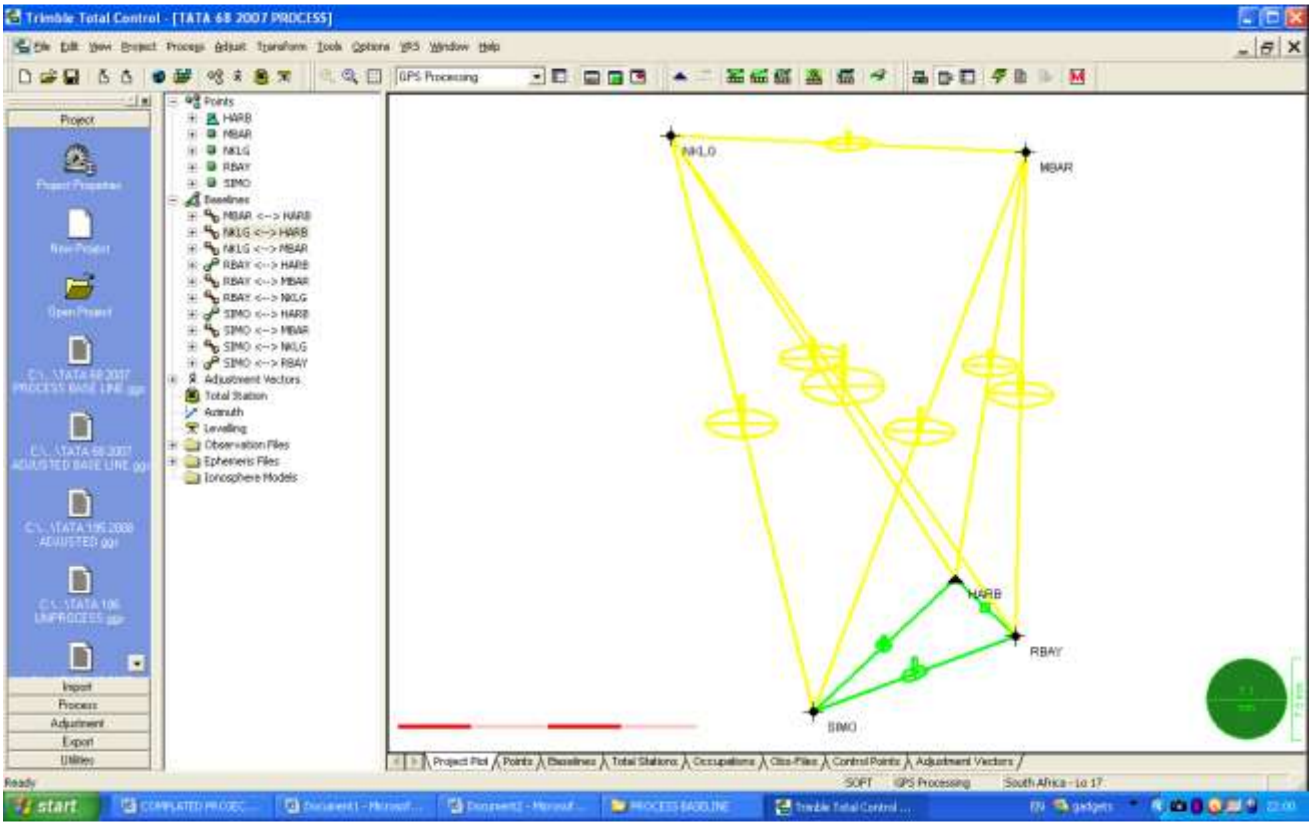

Fig 4.1 Sample of processed baseline for DoY 68 2007

In Figure 4.2 below, shows the adjusted baseline of the network. These baselines that are adjusted are normally indicated with a blue colour. This shows that the baselines have successfully processed and the ambiguity of these baselines resolved because there cycle slip have been reduced to the barest minimum. A 3D biased adjustment in WGS 84 was adopted on these adjusted baselines.

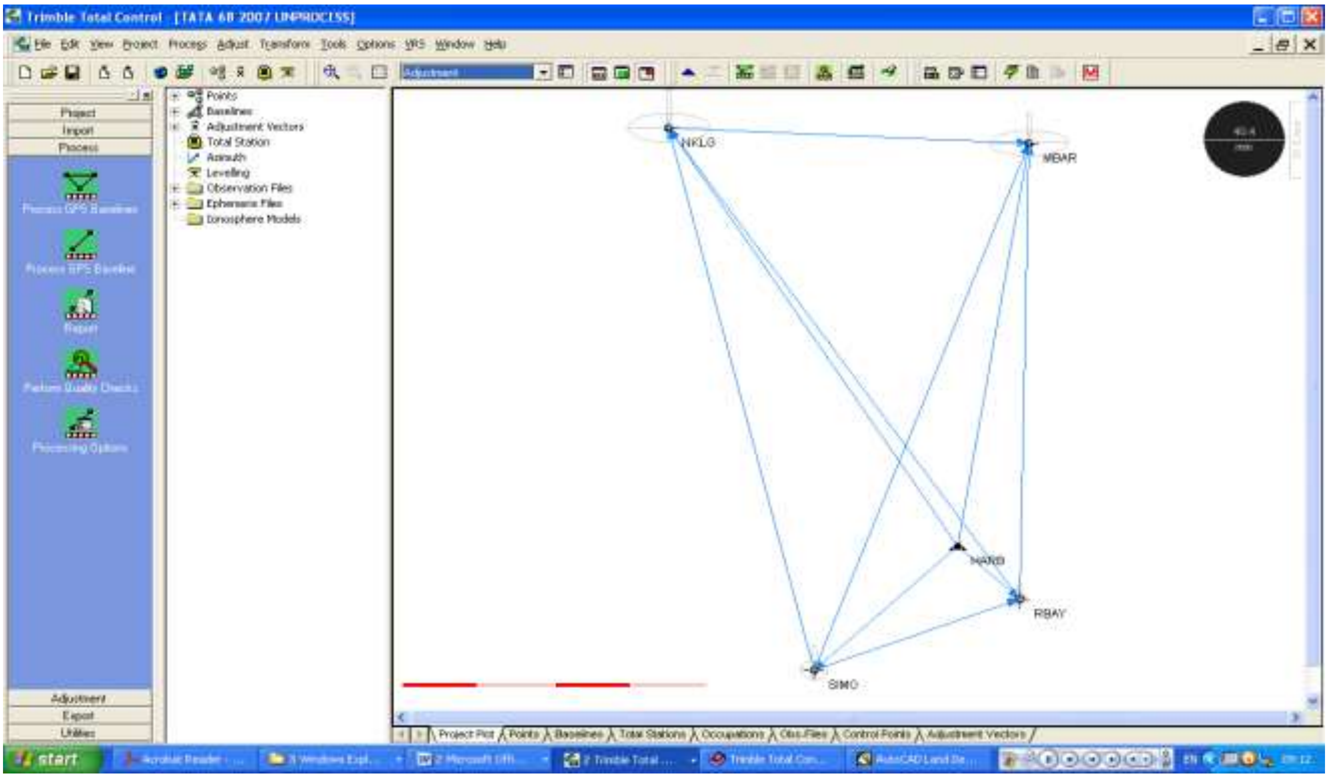

Fig 4.2 Sample of adjusted baseline for DOY 68 in 2007

In table 4.4 below, shows the Comparison of the approximate positions in ITRF 2000 with the mean of the processed positions for DoY 12, 44, 68 in 2007.

A comparison of the approximate positions and the processed positions was carried out to observe if there are deviations between them. Table 4.4 shows that, harb station have the mean difference of 0.009m in the northing, -0.0206m in the Easting and -0.0017m in height.The result also shows that, station nklg have the highest mean difference of 0.639m in the Northing; the Easting has 0.0058m while Height has 0.4437m. The increased or decreased in value all depend on the length of the baseline of that station and the number of the satellite available at that particular time the data are captured.

In terms of there standard deviations, the lowest standard deviation is that of station rbay having 0.0152m,in the Northing, the Easting has 0.0168m while

Height has 0.0079m. nklg station have the highest standard deviation 0.0237m in the northing, 0.0262m in the Easthings and Height as 0.0107m.

Table 4.4 showing positions Comparison for the 2007

	Approximate positions in ITRF 2000 (m)			**Mean of the Processed positions (m)**			**Mean Difference (m)**			**Mean Standard Division(m)**		
Station ID	**Northing**	**Easting**	**Height**	**Northing**	**Easting**	**Height**	**Northing**	**Easting**	**Height**	**Northing**	**Easting**	**Height**
Harb	5084658	2670325	-2768481	5084658.01	2670324.979	-2768481.002	0.0099	-0.0206	-0.0017	0	0	0
Mbar	5482951.388	3260442.643	-66519.849	5482951.869	3260442.559	-66519.58523	0.4811	-0.0843	0.2637	0.0213	0.0249	0.0097
Nklg	6287385.872	1071574.413	39132.764	6287386.512	1071574.419	39133.20777	0.6396	0.0058	0.4437	0.0237	0.0262	0.0107
Rbay	4739765.812	2970758.377	-3054077.646	4739766.119	2970758.154	-3054077.529	0.3073	-0.2226	0.1163	0.0152	0.0168	0.0079
Simo	5010435.805	1670594.692	-3563732.513	5010436.01	1670594.422	-3563732.328	0.2051	-0.2702	0.1843	0.0160	0.0178	0.0084

In table 4.5, shows the Comparison of the approximate positions in ITRF 2000 with the mean of the processed positions for DoY 186 and 195 in 2008.

A comparison of the approximate positions and the processed positions was carried out to observe if there are deviations between them. Table 4.6 shows that, harb station have the mean difference of 0.009m in the northing, -0.0206m in the Easting and -0.0017m.The result also shows that, station mbar have the highest mean difference of 0.0147m in the Northing; the Easting has 0.0634m while Height has 0.4435m.

In terms of there standard deviations, the lowest standard deviation is that of station rbay having 0.0243m,in the Northing, the Easting has 0.0201mwhile Height has 0.0157m.the result also shows that nklg station have the highest standard deviation 0.0691m in the Northing, 0.0691m in the Easting and Height as 0.0353m.

Table 4.5 showing positions Comparison for the 2008

	Approximate positions in ITRF 2000			**Mean of the Processed positions (m)**			**Mean Difference (m)**			**Mean Standard Division(m)**		
Station ID	**Northing**	**Easting**	**Height**	**Northing**	**Easting**	**Height**	**Northing**	**Easting**	**Height**	**Northing**	**Easting**	**Height**
Harb	5084658	2670325	-2768481	5084658.01	2670324.979	-2768481.002	0.0099	-0.0206	-0.0017	0	0	0
mbar	5482951.388	3260442.643	-66519.8489	5482952.103	3260442.706	-66519.561	0.7147	0.0634	0.4335	0.0506	0.0747	0.0267
Nklg	6287385.872	1071574.413	39132.764	6287386.58	1071574.474	39133.19755	0.7082	0.0614	0.2870	0.0691	0.1052	0.0353
Rbay	4739765.812	2970758.377	-3054077.646	4739766.095	2970758.137	-3054077.512	0.2830	-0.24	0.1333	0.0243	0.0201	0.0157
simo	5010435.805	1670594.692	-3563732.513	5010436.114	1670594.453	-3563732.386	0.3092	-02390	0.1267	0.0256	0.0221	0.0343

In table 4.6, shows the Comparison of the approximate positions in ITRF 2000 with the mean of the processed positions for DoY 001 and 002 in 2009

A comparison of the approximate positions and the processed positions was carried out to observe if there are deviations between them. Table 4.6 shows that, harb station have the mean difference of 0.009m in the northing, -0.0206m in the Easthing and -0.0017m.The result also shows that, station nklg have the highest mean difference of 0.0673m in the Northing; the Easthing has 0.0022m while Height has 0.5065m.

In terms of there standard deviations, the lowest standard deviation is that of station nklg having 0.0136m, in the Northing, the Easting has 0.0185m while up has 0.0064m. the result also shows that mbar station have the highest standard deviation 0.0273m in the northing, 0.0370m in the Easthing and Height as 0.0129m.

Table 4.6 showing positions Comparison for the 2009

	Approximate positions in ITRF 2000 (m)			Mean of the Processed positions (m)			Mean Difference (m)			Mean Standard Division (m)		
Station ID	**Northing**	**Easting**	**Height**	**Northing**	**Easting**	**Height**	**Northin g**	**Easting**	**Up**	**Northing**	**Easting**	**Height**
Harb	5084658	2670325	-2768481	5084658.02	2670324.959	-2768481.003	0.0198	-0.0411	-0.0034	0	0	0
Mbar	5482951.388	3260442.643	-66519.8489	5482951.706	3260442.47	-66519.52255	0.3175	-0.173	0.3263	0.0204	0.0277	0.0096
Nklg	6287385.872	1071574.413	39132.764	6287386.545	1071574.415	39133.2705	0.6730	0.0022	0.5065	0.0273	0.0370	0.0129
Rbay	4739765.812	2970758.377	-3054077.646	4739766.242	2970758.199	-3054077.606	0.43025	-0.1779	0.0394	0.0136	0.0185	0.0064
Simo	5010435.805	1670594.692	-3563732.513	5010436.037	1670594.381	-3563732.339	0.23275	-0.3113	0.1732	0.0170	0.0232	0.0080

4.2 Analysis of Results

4.2.1 **Analysis based on Baseline Residual**

In figure 4.3, 4.4 and 4.5, shows residuals graphs as a sample form harb to nklg in 2007, harb to rbay in 2007 and harb to simo in 2009.

In figure 4.3, is the graph plotted cycle slips (m) against time (sec) for DoY 44 in the 2007 for baseline from harb to nklg. The graph shows that there is a lot of sudden jump between the satellites as a result of cycle slip. This occurs when there is an interruption in a receiver's lock-on to a satellite radio signals. During processing, the cycle slips that were not recovered generated additional satellite arcs. The Ionosphere free carrier phase combination was selected, to eliminate this effect.

In figure 4.4, residual float for DoY 68 in 2007 for baseline from harb to rbay shows that there was no much cycle slip. From the graph, it indicates that from the 00:00hrs to 02:00hrs the jump was much but later decrease from 02:00hrs to 04:00hrs. From 04:00hrs to 14:00hrs there was a smooth movement of the satellites. Approximately from the hour of 15:00 to 16:00 there was no satellite present at particular period.

Figure 4.5 the residual float for DoY 001 in 2009 for baseline from harb to simo shows the movement of satellites in which the ambiguity was resolved. The graph indicates a mixed movement of the satellite. It also indicates that between 00:00hrs and 03:00hrs there was a sudden jump within the satellite also between 09:00hrs to 15:00hrs the jump repeat is self. Approximately, between 23:00hrs to24:00hrs no satellite was visible for that period.

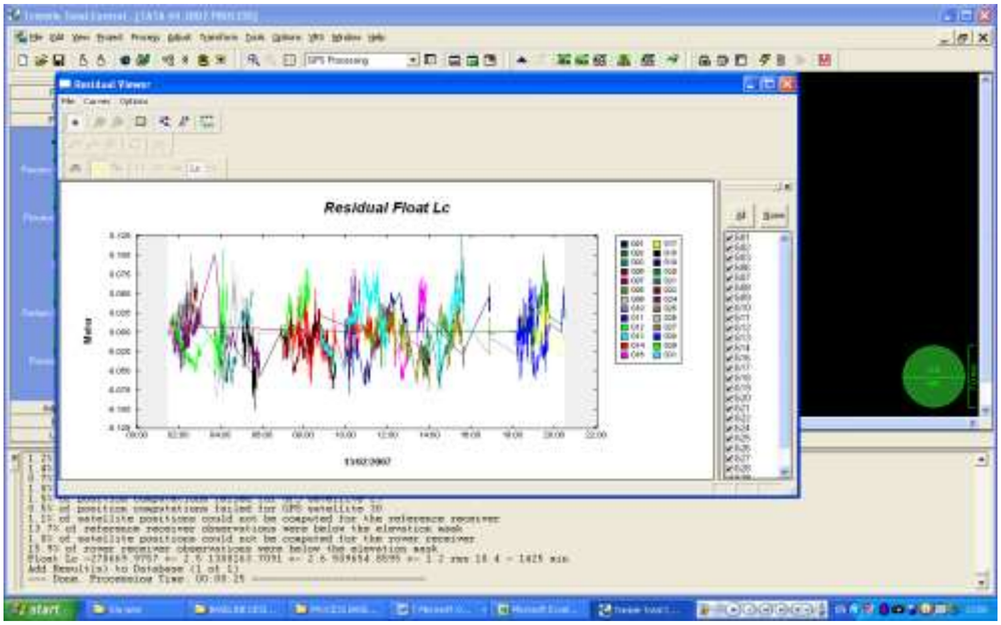

Fig 4.3 Sample of Residual float form harb to nklg for DoY 44 2007

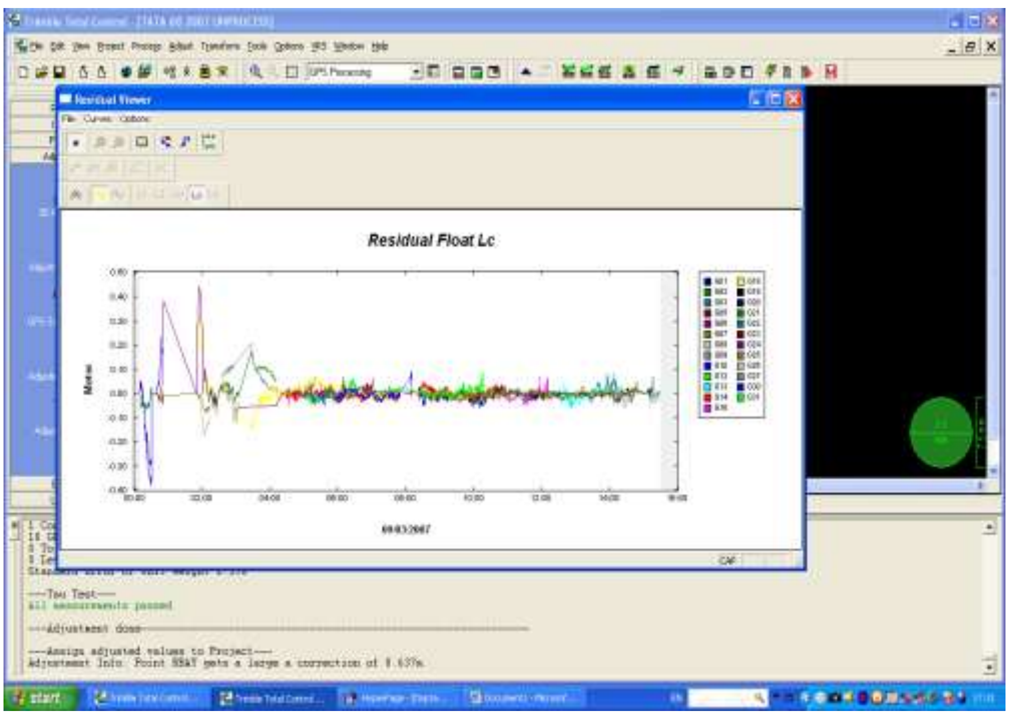

Fig 4.4 Sample of Residual float form harb to rbay for DoY 68 in 2007

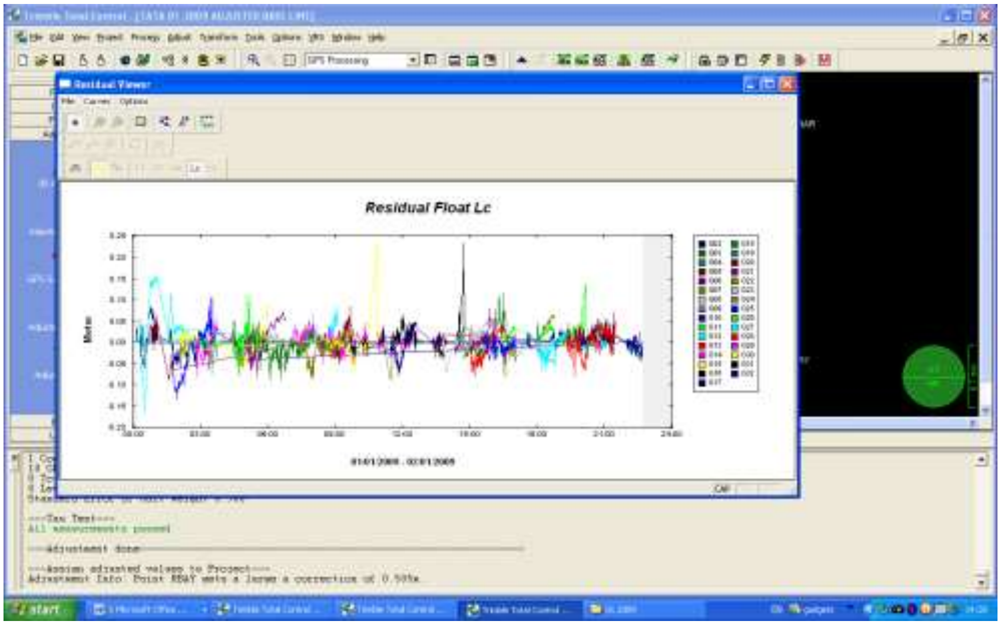

Fig 4.5 Sample of Residual float form harb to simo for DoY 01 in 2009

Station ID	2007		2008		2009	
	Highest value (m)	Lowest value m)	Highest value (m)	Lowest value (m)	Highest value (m)	lowest value (m)
harb-mbar	0.250	-0.275	0.069	-0.057	0.57	-0.63
harb – nklg	0.350	-0.500	0.120	-0.800	0.090	-0.900
harb – rbay	0.100	-0.100	00	00	0.400	-0.500
harb – simo	0.150	-0.150	00	00	0.125	-0.025

Table 4.6 Residual values

Table 4.3 shows sample data of residual float for some DoY 12 in 2007, 186 in 2008 and 001 in 2009. From the analysis made, the results indicate that, the baseline length from harb to rbay in all the years has the smallest values in both the positive and negative direction. In the positive direction, the value is 0.100m and in the negative the value is -0.100 in 2007. In 2008 the value read 0.000m in both directions which indicate that, the baseline hard a fix solution. In the year 2009, the values were 0.400m and -0.500m. This is as the result of short baseline length from harb to rbay the baseline length is in table 4.2. From the table above, it also indicate that harb to nklg has the longest baseline length compared to other baseline length. In 2007, the values in the positive direction read 0.350m and -0.500 in the negative direction. Also in 2008, the values read 0.120 and -0.800 in 2009 the values were 0.090m and -0.900.

There fore, from the above analysis the result shows that, the longer the baseline length, the more it is affected by the atmospheric error and the more the residual float values. Also the shorter the baseline length, the less the atmospheric error, with less the residual float values. This indicate the shorter baseline length have better result than the longer baseline length.

4.2.2 Analysis based on positions Differences

The final positions generated from processing are presented in terms of differences in the Northing, Easting and Height coordinate axes. The standard deviations are computed with reference to the known coordinate of the GNSS stations. The formula for the Standard Deviation is by (Olaitan and Ndomi, 2000)

$$SD = \sqrt{\frac{\sum_{i=1}^{n}(X_i - \bar{X})^2}{n-1}}$$

Where

SD = Standard Deviation

X = Easting or Northing of each station

$\bar{X}$ = Mean or average of Easting or Northing of each station

n = Number of coordinate for each station

Table 4.7 Mean standard deviations of the years

	2007			2008			2009		
Station ID	**Northing**	**Easting**	**Height**	**Northing**	**Easting**	**Height**	**Northing**	**Easting**	**Height**
Harb	0	0	0	0	0	0	0	0	0
Mbar	0.0213	0.0262	0.0097	0.0506	0.0747	0.0267	0.0204	0.0277	0.0096
Nklg	0.0237	0.0249	0.0107	0.0691	0.1052	0.035	0.0273	0.0370	0.0129
Rbay	0.0152	0.0178	0.0079	0.0243	0.0201	0.0157	0.0136	0.0185	0.0064
Simo	0.0160	0.0168	0.0084	0.0256	0.0221	0.0353	0.0170	0.0232	0.0080

From the analysis presented in Table 4.7; the mean standard deviation for the year 2007 and 2008 reveals that station rbay has the lowest standard deviation in the Northing, Easting and up. This could be due to the fact that, the baseline from harb – rbay is the shortest in the network, which agrees with Dodo and Kamarudin (2008) stating that, short baseline are less susceptible to error in GPS baseline measurement.

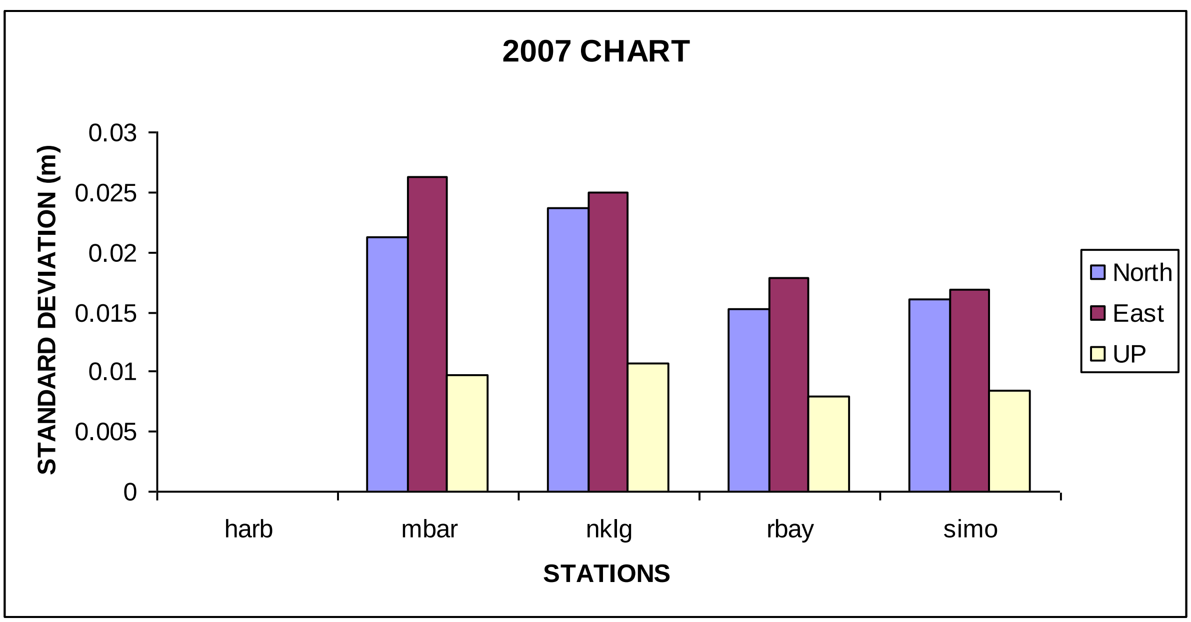

Fig 4.6 showing bar chart for 2007

Fig 4.6 Shows a chart produced for the year 2007. The standard deviation are plotted against there station. The longest bar indicates stations with the highest standard deviation. It is evident from figure 4.6 that, mber has the highest standard deviation of 0.0262m in the Easthing while station nklg has the highest standard deviation 0.0237m in the Northing and 0.0107 in the Height. The figure also reveals that station rbay having the shortest baseline from harb, has the lowest standard deviation.

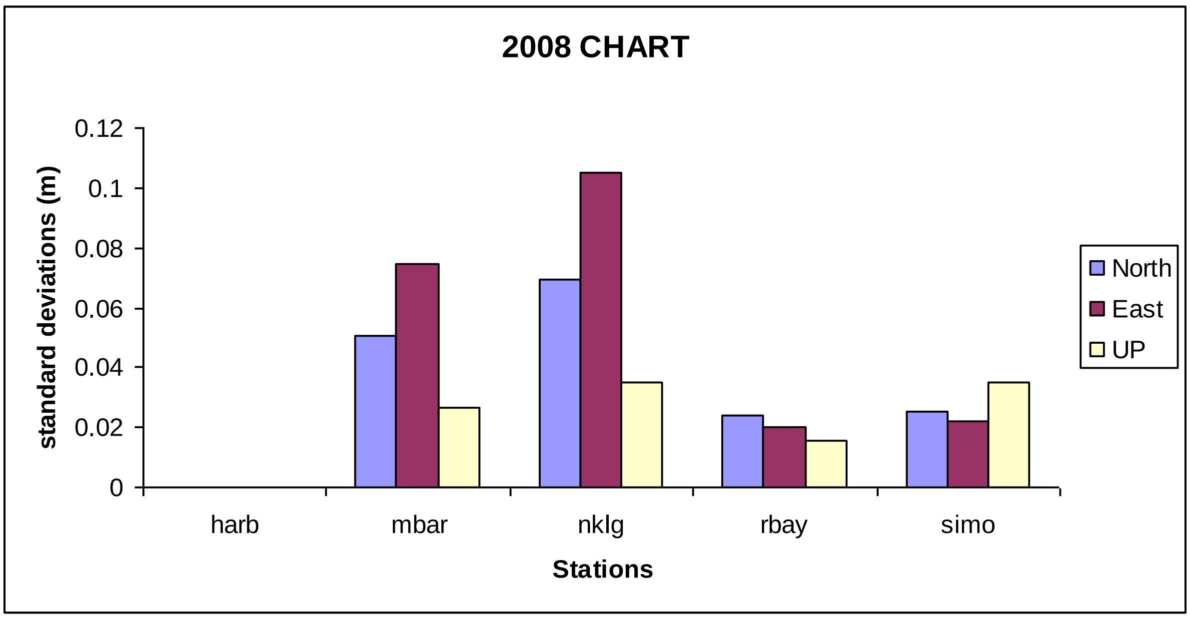

Fig 4.7 showing a bar chart for 2008

Fig 4.7 Shows a chart produced for the year 2008. The standard deviation are plotted against there stations. The longest bar indicates stations with the highest standard deviation. It is evident from figure 4.6 that, nklg has the highest standard deviation of 0.1052m in the Eastings, 0.0691m in the Northings and 0.0355 in the Height. The figure also reveals that station rbay having the shortest baseline from harb, has the lowest standard deviation.

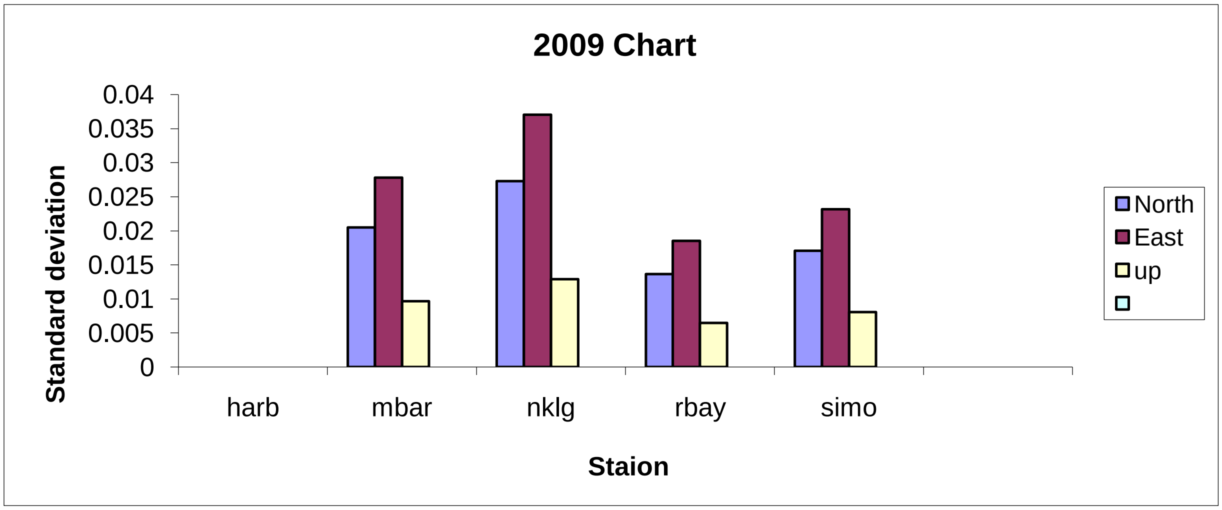

Fig 4.8 showing a chart for 2009

Fig 4.8 Shows a chart produced for the year 2007. The standard deviation are plotted against there station. The longest bar indicates stations with the highest standard deviation. It is evident from figure 4.8 that, mber has the highest standard deviation of 0.0370m in the Eastings, 0.0273m in the Northings and 0.0129m in the Height. The figure also reveals that station rbay having the shortest baseline from harb, has the lowest standard deviation.

CHAPTER 5: CONCLUSIONS AND RECOMMENDATIONS

5.1Conclusions

In this research, attempt was made to assess the positional accuracy of the global navigation satellites system (GNSS) stations in Southern African. The standards deviations of the Stations were obtained after rigorous data processing and analysis.

The analysis on the basis of the baseline residuals reveals that, stations with the longest baseline such as; nklg has the highest standard deviation whereas stations with the lowest baseline such as rbay, has the lowest standard deviation, suggesting that, the shorter the baseline the less the standard deviation hence long baselines are more susceptible to errors than short baseline, thereby having effect on the position of the GNSS stations.

Further analysis was carried out to compare the given or known positions of the stations to the processed positions. The overall result shows no difference in the positions. The standard deviation in all cases range between 0.0064m and 0.0747m. These suggest that, the GNSS stations are in-situ, hence has not undergone distortion that will affect surveying and mapping when used.

5.2 Contributions to the knowledge.

This research work has shown the reliability of the GNSS stations in the study area.

5.3 Recommendations.

It is therefore recommended that:

1. The GNSS stations after installations can be used for any meaningful surveying jobs.
2. Proper GPS planning should be carried out before any GPS work is done so as to know the actual time the Satellite are available for proper transmission of signals.
3. The countries that are in the augmentation of the GNSS station should try as much as possible to reduce the distance between these stations so as to avoid much atmospheric errors.
4. For further research, it is recommended that further work should be done on the long baseline so as to see how it can have a fixed solution after processing.

REFRENCES

Agnew, D.C. and Larson, K.M. (2007): "Finding the repeat times of the GPS constellation" *GPS Solutions* (Springer) 11 (1): 71–76. doi:10.1007/s10291-006-0038-4.

Beutler, G., Moore, A.W.and Mueller, I.I., 2008: "The international global navigation satellite systems service (IGS): development and achievements". Received: 5 March 2008 / Accepted: 1 September 2008 © Springer-Verlag 2008 J.Geod (2009) 83:297-307, Do1 10:1007/s00190-008-0268-Z Original article

Combrinck, L. 2002: "The IGS Network in Africa" an update and real-time issues. Hartebeesthoek Radio Astronomy Observatory, South Africa: IGS Canada (2002) the HartRAO space Geodesy Programme

Chai-Chyang, C., and ching, L. T. (1999): "Testing on tropospheric modeling for GPS tracking station in Taiwan" Geomatics Research Australia 1999 page 77-94

Dodo, J.D and Kamarudin M.N. (2007): "The implementation of global Navigation satellite System (GNSS) in Africa": a proposal for EGNOS Extension and Institutional Framework in: International conference on adaptive science and technology, ICAST, China. A peer-Reviewed Article: ISSN: o855-8906 ISBN: 1921047488pp321-23

Dodo, J.D, and Ono, M.N. (2007): "An evaluation of the Global Navigation Satellite System (GNSS)" Ground infrastructure in Africa, in proceeding of the 1st International Academy of Astronautics Africa regional conference Abuja, Nigerian

Dodo, J.D., Kamarudin, M.N and Yahaya, M.N 2008: "Investigation on the impact of Tropospheric delay on GPS height variation near the equator" A journal of information and communication technology vol.4 No 3, 73-79 ISSN:1449-2679

Dodo, J.D and Kamarudin, M.N, (2007): "Expand the Global navigation Satellite Service to Africa: case of GENOS. In Proceeding of Map Asia 2007 Kuala Lumpur pp No 22

Dodo, J.D and Kamarudin, M.N (2007): "The influence of Different Global tropospheric models baseline precision in local GPS network": case of the Malaysian Johor RTKnet. In: Proceeding of the joint International Symposium on GPS/GNSS boundless opportunities in GNSS and Geoinformatics technologies. Persada Johor, Malaysia. Paper N0.60

de Jong, C.D., Lachapelle, G., Skone, S. and Elema, I.A. (2002): Hydrography, DUP Blue Print, Delft University Press, The Netherlands.

Farahy, H.O., Kamamia, C.M., and Ottichillo, W.K., 2006: "A Common and modern African Geodetic Reference System". Regional Centre for Mapping of Resources for Development Ruaraka, Nairobi

Groenewald, H. 2005: "GNSS approaches rnav (GNSS) implementation in south Africa "Principal Flight Procedures Specialist: ATNS

IGS (2004): IGS Product Table. International GPS Service, http://igscb.jpl.nasa.gov/components/prods.html, extract on 14 Jan 2005.

Kaplan, E. (1996): "Understanding GPS principles and applications", Artech House, Norwood, Mass., USA

Kaplan, E.D., Leva, J.L., and Pavloff, M.S. (1996): "Understanding GPS: Principles and Applications", Chapter 2: Fundamentals of Satellite Navigation, Artech House, Boston, pp: 15-57.

Klobuchar, J.A., (1996): "Global Positioning System: Theory and Applications", Volume I, Chapter 12: Ionospheric Effects on GPS, American Institute of Aeronautics and Astronautics, Inc., Washington D.C., USA, pp: 485-516.

Lachapelle, G. (2001): "Advanced GPS theory and application", EGNO 625 Course Lecture Notes, 2001, University of Calgary, Calgary, Canada.

Leva, J.L., de Haag, M.U. and Dyle, K.V. (1996): "Understanding GPS: Principles and Applications", Chapter 7: Performance of Standalone GPS, Artech House, Boston, pp:237-320.

Lui, Z. (2004): "Ionosphere Tomographic Modeling and Applications Using Global Positioning System (GPS) Measurements", PhD Thesis, UCGE Report Number 20198, Department of Geomatics Engineering, University of Calgary, Canada

Lachapelle, G. (2003): "Advanced GPS – Theory and Applications", EGNO625 Lecture Notes, Department of Geomatics Engineering, University of Calgary

Moore, T., (1997): "An introduction to Differential GPS" Institute of Engineering surveying and space geodesy.University of Nottinham, Nottingham, United Kingdom

Musa, A.A., (2003): "the role of digital technology in surveying" A seminar paper presented at the Nigerian Institute of surveying student week. Federal university of Technology Yola (Unpublished)

Nottingham Scientific Limited, 2005: "The Evolving GNSS a Report to the European Space Agency NSL, final report, and version 1-0 may 2005

Ndukwe, K. N., (2001): "Digital technology in surveying and mapping"Principles, Applications and legislature Issues First publish 2001 by Rhyce kerex publisher, 56, moorhouse Denton street ogui, Enugu, Nigeria.

Olaitan, S.O. and Ndomi, B.M., (2000): "Vocametrics, A High – Tech Problem Solving Quantitative Text with Computer skills" first publish in 2000 by: cape publishers international limited

Onyeka, C.E (2007): "Geoinformatics in Enviromental Monitoring" First published 2007 by san press LTD. ISBN:978-2937-73

Parkinson, B.W. and Enge, P. (1996): "Global Positioning System: Theory and Applications" Volume II, Chapter 1: Differential GPS, American Institute of Astronautics and Aeronautics, Inc., Washington D.C., USA, pp: 3-49.

Pakinson, Spilker (1996): "The Global Positioning System" American Institude of Aeronautics and Astronautics ISBN 9781563471063

PosiTim, (2009): "High Accuracy Global navigation Satellite System (GNSS) Solution and Services", http://www.positim.com/others.htm. page generated September 2009. Last update September 2009. (Last accessed: 7th/01/2010)

Ray, J., (2000): "Mitigation of GPS Code and carrier Phase multipath Effects Using a Multi-Antenna System" PhD Thesis, UCGE Report Number 20136, Department of Geomatics Engineering, University of Calgary, Canada

Roberts, C, (2004): "Improved atmospheric modeling for large scale high- precision positioning based on GNSS CORS Network in Australia" presented at the 2004 International symposium on GNSS/GPS. Sydney Australia 6-8 of December 2004

Sigrist, P. Coppin P. and M. Hermy, (1999**):** "Impact of forest canopy on quality and accuracy of GPS measurement". Publication in: international Journal of Remote sensing vol 20 issue 18, December 1999, page 3595-3610

Skone, S., (1998): "Wide Area Ionosphere Grid Modelling in the Auroral Region", PhD Thesis, UCGE Report Number 20123, Department of Geomatics Engineering, University of Calgary, Calgary, Canada.

Skone, S., (2003): "Atmospheric Affects on Satellite Navigation Systems" ENGO 633 Lecture Notes, Department of Geomatics Engineering, University of Calgary, 2001.

Tagul, A.M, Lim, S. Yam, T. and Rizos, C. (2006): "Mitigation of Distance dependent Error, for GPS Network Positioning" International Global Navigation Satellite System Soceity (IGNSS) Symposium, surface paradise, Australia.

Walpersdorf, A. Bouin, M.-N. Bock, O. and Doerflinger, E., (2007): "Assessment of GPS data for meteorological applications over Africa": Study of error sources and analysis of positioning accuracy. A Journal of Atmospheric and Solar- Terrestral Physic 69 (2007) 1312-133

Wyllie, S.J., and Zhang, K.F, (2003): "A comparison of Ionospheric models for precise positioning in Victoria": Presented at SatNav 2003.
The 6th international symposium on satellite Navigation Technology Including Mobile positioning and location services Melbourne, Australia 22-25 July 2003

Yahya, M.H. and Kamarudin, M.N. (2007) "The impact of tropospheric delay towards the accuracy of GPS height determination" In: Proceeding of the Joint International Symposium on GPS/GNSS boundless opportunities in GNSS and Geo-informatics technologies. Persada Johor, Malaysia. Paper N0.60

Yaw, and Günter's, (2006): "Framework for the establishment of a Nationwide Network Global Navigation Satellite System (GNSS)", a cost effective tool for land Development in Ghana.

http://www.bere-gnss_solution.com/link//.html: (last accessed 7th/01/2010)

http://spot.colorado.edu/~kristine/gpsrep.pdf :(last accessed 23/03/2010)

http://www.sopac.ucsd.edu/: (last accessed 6th/05/2010)

http://www.igscb.jpl.nasa.gov: (last accessed 6th/05/2010)

http://www.ngs.noaa.gov: (last accessed 17th/10/2010)

APPENDIX

Appendix A: showing 3D Network Adjustment for Day of the year 12 in 2007

Trimble

3D Network Adjustment for Day of the year 12 in 2007

www.trimble.com

Project : M.TECH THESIS

User Name	Tata Herbert	**Date & Time**	12:24:59 14/07/2010
Coordinate System	South Africa	**Zone**	Lo 17
Project Datum	Cape	**Geoid Model**	EGM96 (Global)
Coordinate Units	Meter		
Distance Units	Meter		
Height Units	Meter		
Angle Units	Degrees		

Network Adjustment in WGS84.	
Number of GPS Baselines	10
Number of Total Station Measurements	0
Number of Control Points in WGS84	1
Number of Adjusted Points	5
Confidence level	1 σ
Significance Level for Tau Test	1.00 %
Standard Error of Unit Weight	0.646
Number of Iterations	1
Refraction Coefficient	0.140

- Observations which were rejected by the statistical test are marked.

1.   Baselines Input in WGS84 (Components and Std.Dev.)

Observation	ΔXm	σmm	ΔYm	σmm	ΔZm	σmm	Solution
HARB-MBAR	398293.7772	36.2	590117.5926	43.2	2701961.6364	14.6	Double Diff. / Float / Lc
HARB-NKLG	1202728.4457	40.3	-1598750.7482	51.1	2807614.4770	18.4	Double Diff. / Float / Lc
HARB-RBAY	-344891.8683	21.1	300433.1958	24.6	-285596.5713	11.1	Double Diff. / Float / Lc
HARB-SIMO	-74221.8478	26.4	-999730.6029	32.5	-795251.4804	13.7	Double Diff. / Float / Lc
NKLG-MBAR	-804434.6534	31.4	2188868.3049	39.1	-105652.8048	14.7	Double Diff. / Float / Lc
RBAY-MBAR	743185.6020	37.6	289684.4382	47.9	2987558.1894	15.9	Double Diff. / Float / Lc
RBAY-NKLG	1547620.3097	48.6	-1899183.9053	62.3	3093211.0483	21.3	Double Diff. / Float / Lc
SIMO-MBAR	472515.6381	42.6	1589848.1792	57.8	3497213.1063	19.2	Double Diff. / Float / Lc
SIMO-NKLG	1276950.3318	48.7	-599020.1236	61.8	3602865.9367	21.2	Double Diff. / Float / Lc
SIMO-RBAY	-270670.0141	22.0	1300163.7891	26.3	509654.9176	11.0	Double Diff. / Float / Lc

- Standard deviations of the static baselines have been multiplied with the factor 10.00.

2. WGS84 Control Points Input (Cart. Coordinates and Std.Dev.)

Point	X	σ	Y	σ	Z	σ
HARB	5084655.2770m	0.0mm	2670325.0330m	0.0mm	-2768481.1986m	0.0mm

3. Adjusted Baselines in WGS84 (Components and Std.Dev.)

Observation	ΔX	σ	ΔY	σ	ΔZ	σ
HARB-MBAR	398293.7740m	13.9mm	590117.5920m	17.2mm	2701961.6372m	6.1mm
HARB-NKLG	1202728.4456m	15.0mm	-1598750.7265m	18.8mm	2807614.4616m	6.9mm
HARB-RBAY	-344891.8630m	10.6mm	300433.1878m	12.6mm	-285596.5665m	5.3mm
HARB-SIMO	-74221.8541m	11.6mm	-999730.5997m	14.2mm	-795251.4798m	5.8mm
NKLG-MBAR	-804434.6716m	14.8mm	2188868.3185m	18.6mm	-105652.8244m	6.7mm
RBAY-MBAR	743185.6369m	14.0mm	289684.4042m	17.4mm	2987558.2036m	6.2mm
RBAY-NKLG	1547620.3086m	15.2mm	-1899183.9143m	19.1mm	3093211.0280m	6.9mm
SIMO-MBAR	472515.6281m	14.5mm	1589848.1917m	18.3mm	3497213.1170m	6.5mm
SIMO-NKLG	1276950.2997m	15.6mm	-599020.1268m	19.7mm	3602865.9414m	7.2mm
SIMO-RBAY	-270670.0089m	10.9mm	1300163.7875m	13.3mm	509654.9134m	5.4mm

4.   Baseline Residuals (Residuals and Standardized Residuals)

Observation	Northing Res.	Stand. Res.	Easting Res.	Stand. Res.	Height Res.	Stand. Res.	Red.No.
HARB-MBAR	-0.7mm	-0.078	0.9mm	0.039	-3.2mm	-0.207	1.85
HARB-NKLG	-9.5mm	-0.853	19.2mm	0.713	15.7mm	0.753	2.02
HARB-RBAY	4.8mm	1.050	-9.6mm	-0.942	-1.2mm	-0.153	1.22
HARB-SIMO	-1.3mm	-0.187	5.8mm	0.354	-3.9mm	-0.344	1.66
NKLG-MBAR	-21.9mm	-2.941	20.5mm	1.060	-0.3mm	-0.026	1.37
RBAY-MBAR	19.4mm	1.980	-46.3mm	-1.766	7.4mm	0.405	1.99
RBAY-NKLG	-20.5mm	-1.396	-7.4mm	-0.214	4.2mm	0.156	2.29
SIMO-MBAR	8.2mm	0.766	15.7mm	0.475	-7.4mm	-0.332	2.18
SIMO-NKLG	-8.8mm	-0.710	12.1mm	0.354	-29.0mm	-1.044	2.22
SIMO-RBAY	-2.1mm	-0.483	-3.8mm	-0.342	5.3mm	0.638	1.21

5.   Adjusted Points in WGS84 (Cart. Coordinates and Std.Dev.)

Point	X	σ	Y	σ	Z	σ
HARB	5084655.2770m	0.0mm	2670325.0330m	0.0mm	-2768481.1986m	0.0mm
MBAR	5482949.0510m	13.9mm	3260442.6250m	17.2mm	-66519.5614m	6.1mm
NKLG	6287383.7226m	15.0mm	1071574.3065m	18.8mm	39133.2630m	6.9mm
RBAY	4739763.4140m	10.6mm	2970758.2208m	12.6mm	-3054077.7651m	5.3mm
SIMO	5010433.4229m	11.6mm	1670594.4333m	14.2mm	-3563732.6784m	5.8mm

6.   Adjusted Points in WGS84 (Geogr. Coordinates and Std.Dev.)

Point	Latitude	σ	Longitude	σ	Height	σ
HARB	S 25° 53' 13.09806"	0.0mm	E 27° 42' 26.11718"	0.0mm	1556.2000m	0.0mm
MBAR	S 0° 36' 05.27989"	6.1mm	E 30° 44' 16.39245"	18.1mm	1335.6329m	12.7mm
NKLG	N 0° 21' 14.07545"	6.9mm	E 9° 40' 19.65372"	19.2mm	29.4530m	14.4mm
RBAY	S 28° 47' 44.00151"	5.6mm	E 32° 04' 42.22838"	13.1mm	29.9973m	9.7mm
SIMO	S 34° 11' 16.62732"	6.7mm	E 18° 26' 22.48645"	14.8mm	37.6475m	10.3mm

7.   Adjusted Points Error Ellipses

Point	Semimajor Axis	Semiminor Axis	Angle	95% confidence radius
HARB	0.0mm	0.0mm	90.0°	0.0mm
MBAR	18.1mm	6.1mm	-88.4°	36.0mm
NKLG	19.2mm	6.8mm	-88.3°	38.3mm
RBAY	13.1mm	5.6mm	89.7°	26.4mm
SIMO	14.8mm	6.6mm	-85.5°	29.9mm

Appendix B: showing 3D Network Adjustment for Day of the year 44 in 2007

Trimble ***3D Network Adjustment for Day of the year 44 in 2007***

Project : Untitled1

User Name	Tata Herbert	**Date & Time**	11:44:20 12/07/2010
Coordinate System	South Africa	**Zone**	Lo 17
Project Datum	Cape	**Geoid Model**	EGM96 (Global)
Coordinate Units	Meter		
Distance Units	Meter		
Height Units	Meter		
Angle Units	Degrees		

Network Adjustment in WGS84.	
Number of GPS Baselines	10
Number of Total Station Measurements	0
Number of Control Points in WGS84	1
Number of Adjusted Points	5
Confidence level	1 σ
Significance Level for Tau Test	1.00 %
Standard Error of Unit Weight	1.106
Number of Iterations	1
Refraction Coefficient	0.140

- Observations which were rejected by the statistical test are marked.

1. Baselines Input in WGS84 (Components and Std.Dev.)

Observation	ΔXm	σmm	ΔYm	σmm	ΔZm	σmm	Solution
HARB-MBAR	398294.0926	34.8	590117.7592	39.6	2701961.3058	15.7	Double Diff. / Float / Lc
HARB-NKLG	1202728.8727	43.6	-1598750.3779	56.1	2807614.0944	20.3	Double Diff. / Float / Lc
HARB-RBAY	-344891.7175	22.0	300433.2466	22.8	-285596.6173	11.3	Double Diff. / Float / Lc
HARB-SIMO	-74221.7150	21.3	-999730.4307	26.1	-795251.4810	11.7	Double Diff. / Float / Lc
NKLG-MBAR	-804434.7528	35.2	2188868.1336	46.3	-105652.7848	16.6	Double Diff. / Float / Lc
RBAY-MBAR	743185.9982	62.4	289684.5684	67.5	2987557.8162	29.7	Double Diff. / Float / Lc
RBAY-NKLG	1547620.6775	74.3	-1899183.6947	84.3	3093210.6444	32.4	Double Diff. / Float / Lc
SIMO-MBAR	472515.7861	51.9	1589848.3006	53.7	3497212.7665	22.0	Double Diff. / Float / Lc
SIMO-NKLG	1276950.5405	56.3	-599019.9234	68.5	3602865.5911	24.0	Double Diff. / Float / Lc
SIMO-RBAY	-270669.9749	24.2	1300163.6863	27.7	509654.8613	12.7	Double Diff. / Float / Lc

- Standard deviations of the static baselines have been multiplied with the factor 10.00.

2. WGS84 Control Points Input (Cart. Coordinates and Std.Dev.)

Point	X	σ	Y	σ	Z	σ
HARB	5084658.0198m	0.0mm	2670324.9589m	0.0mm	-2768481.0034m	0.0mm

3. Adjusted Baselines in WGS84 (Components and Std.Dev.)

Observation	ΔX	σ	ΔY	σ	ΔZ	σ
HARB-MBAR	398294.1095m	26.0mm	590117.7854m	30.0mm	2701961.2922m	11.9mm
HARB-NKLG	1202728.8671m	28.7mm	-1598750.3715m	36.0mm	2807614.0835m	13.2mm

HARB-RBAY	-344891.7220m	19.0mm	300433.2471m	20.6mm	-285596.6087m	9.7mm
HARB-SIMO	-74221.7208m	18.2mm	-999730.4459m	21.6mm	-795251.4801m	9.5mm
NKLG-MBAR	-804434.7576m	28.9mm	2188868.1570m	36.9mm	-105652.7913m	13.2mm
RBAY-MBAR	743185.8316m	28.8mm	289684.5383m	32.5mm	2987557.9009m	13.5mm
RBAY-NKLG	1547620.5892m	31.2mm	-1899183.6187m	37.9mm	3093210.6922m	14.4mm
SIMO-MBAR	472515.8303m	27.9mm	1589848.2313m	32.0mm	3497212.7723m	12.9mm
SIMO-NKLG	1276950.5880m	30.2mm	-599019.9257m	37.4mm	3602865.5636m	13.8mm
SIMO-RBAY	-270670.0012m	19.9mm	1300163.6930m	22.7mm	509654.8714m	10.3mm

4. Baseline Residuals (Residuals and Standardized Residuals)

Observation	Northing Res.	Stand. Res.	Easting Res.	Stand. Res.	Height Res.	Stand. Res.	Red.No.
HARB-MBAR	-0.4mm	-0.028	15.3mm	0.447	30.4mm	1.252	1.62
HARB-NKLG	-10.7mm	-0.551	8.2mm	0.153	3.0mm	0.087	1.96
HARB-RBAY	6.1mm	0.938	2.6mm	0.161	-7.1mm	-0.495	1.10
HARB-SIMO	-4.5mm	-0.426	-10.7mm	-0.557	-11.4mm	-0.829	1.33
NKLG-MBAR	-3.0mm	-0.170	22.9mm	0.609	8.8mm	0.446	1.39
RBAY-MBAR	5.6mm	0.244	50.9mm	0.700	-182.3mm	-3.065	2.41
RBAY-NKLG	24.2mm	0.961	108.4mm	1.136	-59.4mm	-0.896	2.46
SIMO-MBAR	8.2mm	0.389	-81.9mm	-1.481	3.7mm	0.084	2.18
SIMO-NKLG	-6.8mm	-0.300	-24.1mm	-0.344	48.9mm	1.000	2.23
SIMO-RBAY	0.3mm	0.038	18.2mm	0.770	-22.6mm	-1.490	1.29

5. Adjusted Points in WGS84 (Cart. Coordinates and Std.Dev.)

Point	X	σ	Y	σ	Z	σ
HARB	5084658.0198m	0.0mm	2670324.9589m	0.0mm	-2768481.0034m	0.0mm
MBAR	5482952.1293m	26.0mm	3260442.7443m	30.0mm	-66519.7112m	11.9mm
NKLG	6287386.8869m	28.7mm	1071574.5873m	36.0mm	39133.0801m	13.2mm
RBAY	4739766.2977m	19.0mm	2970758.2060m	20.6mm	-3054077.6121m	9.7mm
SIMO	5010436.2989m	18.2mm	1670594.5130m	21.6mm	-3563732.4835m	9.5mm

6. Adjusted Points in WGS84 (Geogr. Coordinates and Std.Dev.)

Point	Latitude	σ	Longitude	σ	Height	σ
HARB	S 25° 53' 13.05840"	0.0mm	E 27° 42' 26.06902"	0.0mm	1558.2684m	0.0mm
MBAR	S 0° 36' 05.28384"	11.9mm	E 30° 44' 16.34489"	32.3mm	1338.3411m	23.1mm
NKLG	N 0° 21' 14.06885"	13.2mm	E 9° 40' 19.64548"	37.4mm	32.6183m	26.9mm
RBAY	S 28° 47' 43.95905"	9.0mm	E 32° 04' 42.17145"	22.5mm	32.0580m	17.1mm
SIMO	S 34° 11' 16.57187"	10.7mm	E 18° 26' 22.45388"	22.7mm	39.8157m	16.0mm

7. Adjusted Points Error Ellipses

Point	Semimajor Axis	Semiminor Axis	Angle	95% confidence radius
HARB	0.0mm	0.0mm	0.0°	0.0mm
MBAR	32.3mm	11.9mm	89.9°	64.5mm
NKLG	37.4mm	13.2mm	89.9°	74.5mm
RBAY	22.5mm	9.0mm	88.2°	45.1mm
SIMO	22.8mm	10.6mm	-86.0°	46.1mm

Appendix C: showing 3D Network Adjustment for Day of the year 68 in 2007

3D Network Adjustment for day of the Year 68 in 2007

www.trimble.com

Project : M.TECH THESIS

User Name	Tata Herbert	**Date & Time**	15:25:52 12/07/2010
Coordinate System	South Africa	**Zone**	Lo 17
Project Datum	Cape	**Geoid Model**	EGM96 (Global)
Coordinate Units	Meter		
Distance Units	Meter		
Height Units	Meter		
Angle Units	Degrees		

Network Adjustment in WGS84.	
Number of GPS Baselines	10
Number of Total Station Measurements	0
Number of Control Points in WGS84	1
Number of Adjusted Points	5
Confidence level	1 σ
Significance Level for Tau Test	1.00 %
Standard Error of Unit Weight	1.165
Number of Iterations	1
Refraction Coefficient	0.140

- Observations which were rejected by the statistical test are marked.

1. Baselines Input in WGS84 (Components and Std.Dev.)

Observation	ΔXm	σmm	ΔYm	σmm	ΔZm	σmm	Solution
HARB-MBAR	398293.7268	38.4	590117.5464	43.9	2701961.4550	16.3	Double Diff. / Float / Lc
HARB-NKLG	1202728.4840	46.3	-1598750.5551	51.2	2807614.2464	19.1	Double Diff. / Float / Lc
HARB-RBAY	-344891.8545	20.7	300433.1982	22.7	-285596.5602	10.5	Double Diff. / Float / Lc
HARB-SIMO	-74222.1094	24.2	-999730.5841	28.1	-795251.2693	13.0	Double Diff. / Float / Lc
NKLG-MBAR	-804434.7380	29.2	2188868.0839	38.3	-105652.7916	13.9	Double Diff. / Float / Lc
RBAY-MBAR	743185.6664	47.6	289684.4085	47.0	2987557.9657	20.5	Double Diff. / Float / Lc
RBAY-NKLG	1547620.5012	85.8	-1899183.7382	69.3	3093210.7173	31.6	Double Diff. / Float / Lc
SIMO-MBAR	472515.8917	40.7	1589848.1693	45.4	3497212.6608	17.0	Double Diff. / Float / Lc
SIMO-NKLG	1276950.6801	55.2	-599019.9893	58.8	3602865.4551	22.4	Double Diff. / Float / Lc
SIMO-RBAY	-270669.8323	23.5	1300163.7820	27.1	509654.7425	13.3	Double Diff. / Float / Lc

- Standard deviations of the static baselines have been multiplied with the factor 10.00.

2. WGS84 Control Points Input (Cart. Coordinates and Std.Dev.)

Point	X	σ	Y	σ	Z	σ
HARB	5084658.0099m	0.0mm	2670324.9794m	0.0mm	-2768481.0017m	0.0mm

3. Adjusted Baselines in WGS84 (Components and Std.Dev.)

Observation	ΔX	σ	ΔY	σ	ΔZ	σ

HARB-MBAR	398293.7680m	26.4mm	590117.5592m	29.6mm	2701961.4269m	11.6mm
HARB-NKLG	1202728.5195m	30.1mm	-1598750.5471m	33.6mm	2807614.2177m	12.9mm
HARB-RBAY	-344891.8901m	19.3mm	300433.1886m	21.3mm	-285596.5418m	9.7mm
HARB-SIMO	-74222.0936m	20.4mm	-999730.5907m	23.3mm	-795251.2639m	10.4mm
NKLG-MBAR	-804434.7515m	27.3mm	2188868.1064m	33.1mm	-105652.7908m	12.1mm
RBAY-MBAR	743185.6581m	27.8mm	289684.3707m	30.1mm	2987557.9687m	12.4mm
RBAY-NKLG	1547620.4096m	31.8mm	-1899183.7357m	34.6mm	3093210.7595m	13.8mm
SIMO-MBAR	472515.8617m	27.2mm	1589848.1500m	30.3mm	3497212.6908m	12.0mm
SIMO-NKLG	1276950.6131m	31.0mm	-599019.9564m	34.6mm	3602865.4816m	13.5mm
SIMO-RBAY	-270669.7965m	20.6mm	1300163.7793m	23.3mm	509654.7221m	10.8mm

4. Baseline Residuals (Residuals and Standardized Residuals)

Observation	Northing Res.	Stand. Res.	Easting Res.	Stand. Res.	Height Res.	Stand. Res.	Red.No.
HARB-MBAR	-6.7mm	-0.400	-7.8mm	-0.166	50.5mm	1.787	1.94
HARB-NKLG	-10.5mm	-0.513	-9.4mm	-0.177	44.1mm	1.135	2.03
HARB-RBAY	0.9mm	0.122	8.0mm	0.501	-40.5mm	-2.857	1.08
HARB-SIMO	9.6mm	0.841	-13.2mm	-0.552	7.4mm	0.417	1.51
NKLG-MBAR	0.1mm	0.007	26.2mm	0.844	-1.7mm	-0.104	1.25
RBAY-MBAR	-8.2mm	-0.440	-29.6mm	-0.569	-23.7mm	-0.568	2.15
RBAY-NKLG	3.0mm	0.108	44.8mm	0.498	-90.4mm	-1.115	2.51
SIMO-MBAR	11.4mm	0.835	-3.2mm	-0.065	-45.1mm	-1.370	1.91
SIMO-NKLG	4.6mm	0.203	60.3mm	0.963	-51.2mm	-0.977	2.23
SIMO-RBAY	-5.0mm	-0.507	-19.1mm	-0.839	36.4mm	2.137	1.40

5. Adjusted Points in WGS84 (Cart. Coordinates and Std.Dev.)

Point	X	σ	Y	σ	Z	σ
HARB	5084658.0099m	0.0mm	2670324.9794m	0.0mm	-2768481.0017m	0.0mm
MBAR	5482951.7779m	26.4mm	3260442.5387m	29.6mm	-66519.5748m	11.6mm
NKLG	6287386.5293m	30.1mm	1071574.4323m	33.6mm	39133.2160m	12.9mm
RBAY	4739766.1198m	19.3mm	2970758.1680m	21.3mm	-3054077.5434m	9.7mm
SIMO	5010435.9162m	20.4mm	1670594.3887m	23.3mm	-3563732.2656m	10.4mm

6. Adjusted Points in WGS84 (Geogr. Coordinates and Std.Dev.)

Point	Latitude	σ	Longitude	σ	Height	σ
HARB	S 25° 53' 13.05834"	0.0mm	E 27° 42' 26.06984"	0.0mm	1558.2684m	0.0mm
MBAR	S 0° 36' 05.27954"	11.5mm	E 30° 44' 16.34498"	32.7mm	1337.9326m	22.5mm
NKLG	N 0° 21' 14.07336"	13.0mm	E 9° 40' 19.64248"	35.0mm	32.2407m	28.5mm
RBAY	S 28° 47' 43.95977"	9.8mm	E 32° 04' 42.17374"	22.5mm	31.8752m	17.8mm
SIMO	S 34° 11' 16.57336"	11.6mm	E 18° 26' 22.45400"	24.5mm	39.3604m	18.2mm

7. Adjusted Points Error Ellipses

Point	Semimajor Axis	Semiminor Axis	Angle	95% confidence radius
HARB	0.0mm	0.0mm	90.0°	0.0mm
MBAR	32.7mm	11.5mm	88.6°	65.1mm
NKLG	35.0mm	13.0mm	89.0°	69.9mm
RBAY	22.5mm	9.8mm	89.4°	45.4mm
SIMO	24.6mm	11.4mm	-84.7°	49.8mm

Appendix D: showing 3D Network Adjustment for Day of the year 186 in 2008

3D Network Adjustment for day of the Year 186 in 2008

Project : M.TECH THESIS

User Name	Tata Herbert	**Date & Time**	21:18:44 12/07/2010
Coordinate System	South Africa	**Zone**	Lo 17
Project Datum	Cape	**Geoid Model**	EGM96 (Global)
Coordinate Units	Meter		
Distance Units	Meter		
Height Units	Meter		
Angle Units	Degrees		

Network Adjustment in WGS84.	
Number of GPS Baselines	10
Number of Total Station Measurements	0
Number of Control Points in WGS84	1
Number of Adjusted Points	5
Confidence level	1 σ
Significance Level for Tau Test	1.00 %
Standard Error of Unit Weight	4.431
Number of Iterations	1
Refraction Coefficient	0.140

- Observations which were rejected by the statistical test are marked.

1. Baselines Input in WGS84 (Components and Std.Dev.)

Observation	**ΔXm**	**σmm**	**ΔYm**	**σmm**	**ΔZm**	**σmm**	**Solution**
HARB-MBAR	398294.0688	45.6	590117.6779	73.1	2701961.3158	24.1	Double Diff. / Float / Lc
HARB-NKLG	1202728.4870	54.7	-1598750.4595	85.2	2807614.1036	27.4	Double Diff. / Float / Lc
HARB-RBAY	-344891.9168	8.7	300433.1486	6.3	-285596.4972	6.0	Double Diff. / Fixed / Lc
HARB-SIMO	-74221.7937	9.4	-999730.4936	6.8	-795251.4443	9.2	Double Diff. / Fixed / Lc
NKLG-MBAR	-804434.4325	39.9	2188868.2736	55.6	-105652.7948	19.1	Double Diff. / Float / Lc
RBAY-MBAR	743186.2183	31.4	289684.6550	43.3	2987558.0527	15.0	Double Diff. / Float / Lc
RBAY-NKLG	1547620.8095	59.5	-1899183.7886	96.3	3093210.7664	30.5	Double Diff. / Float / Lc
SIMO-MBAR	472516.0977	31.6	1589848.3785	54.4	3497213.0195	17.0	Double Diff. / Float / Lc
SIMO-NKLG	1276950.2171	66.9	-599020.0083	111.4	3602865.6441	32.4	Double Diff. / Float / Lc
SIMO-RBAY	-270670.1244	49.2	1300163.8475	39.9	509654.9705	34.4	Double Diff. / Fixed / Lc

- Standard deviations of the static baselines have been multiplied with the factor 10.00.

2. WGS84 Control Points Input (Cart. Coordinates and Std.Dev.)

Point	**X**	**σ**	**Y**	**σ**	**Z**	**σ**
HARB	5084658.0099m	0.0mm	2670324.9794m	0.0mm	-2768481.0017m	0.0mm

3. Adjusted Baselines in WGS84 (Components and Std.Dev.)

Observation	**ΔX**	**σ**	**ΔY**	**σ**	**ΔZ**	**σ**

HARB-MBAR	398294.2394m	85.2mm	590117.8099m	126.6mm	2701961.4949m	45.2mm
HARB-NKLG	1202728.6236m	120.0mm	-1598750.4958m	184.7mm	2807614.2264m	61.1mm
HARB-RBAY	-344891.9250m	36.8mm	300433.1492m	27.2mm	-285596.5068m	24.9mm
HARB-SIMO	-74221.7884m	39.5mm	-999730.4985m	29.4mm	-795251.4621m	35.3mm
NKLG-MBAR	-804434.3843m	123.1mm	2188868.3058m	184.8mm	-105652.7315m	60.4mm
RBAY-MBAR	743186.1644m	86.3mm	289684.6607m	126.7mm	2987558.0017m	45.2mm
RBAY-NKLG	1547620.5487m	121.1mm	-1899183.6451m	185.0mm	3093210.7332m	61.8mm
SIMO-MBAR	472516.0278m	86.8mm	1589848.3084m	127.8mm	3497212.9570m	48.0mm
SIMO-NKLG	1276950.4120m	122.0mm	-599019.9974m	185.6mm	3602865.6885m	64.0mm
SIMO-RBAY	-270670.1366m	52.0mm	1300163.6477m	39.4mm	509654.9553m	40.6mm

4. Baseline Residuals (Residuals and Standardized Residuals)

Observation	Northing Res.	Stand. Res.	Easting Res.	Stand. Res.	Height Res.	Stand. Res.	Red.No.
HARB-MBAR	253.9mm	2.906	37.6mm	0.127	112.9mm	0.587	2.48
HARB-NKLG	155.9mm	1.504	-95.7mm	-0.278	40.0mm	0.215	2.26
HARB-RBAY	-11.7mm	-1.586	4.4mm	0.633	-2.1mm	-0.173	0.24
HARB-SIMO	-14.9mm	-0.954	-6.8mm	-0.777	10.0mm	0.562	0.39
NKLG-MBAR	82.1mm	1.083	6.0mm	0.035	24.3mm	0.236	1.47
RBAY-MBAR	-65.6mm	-1.275	30.2mm	0.212	-18.3mm	-0.165	1.73
RBAY-NKLG	-101.5mm	-1.011	248.4mm	0.605	-133.2mm	-0.680	2.31
SIMO-MBAR	-97.4mm	-1.862	-29.5mm	-0.151	-57.7mm	-0.454	1.90
SIMO-NKLG	117.5mm	0.925	-80.9mm	-0.167	140.4mm	0.644	2.43
SIMO-RBAY	-59.0mm	-0.479	-171.2mm	-1.134	-86.7mm	-0.360	2.80

5. Adjusted Points in WGS84 (Cart. Coordinates and Std.Dev.)

Point	X	σ	Y	σ	Z	σ
HARB	5084658.0099m	0.0mm	2670324.9794m	0.0mm	-2768481.0017m	0.0mm
MBAR	5482952.2493m	85.2mm	3260442.7894m	126.6mm	-66519.5068m	45.2mm
NKLG	6287386.6335m	120.0mm	1071574.4836m	184.7mm	39133.2247m	61.1mm
RBAY	4739766.0849m	36.8mm	2970758.1287m	27.2mm	-3054077.5085m	24.9mm
SIMO	5010436.2215m	39.5mm	1670594.4809m	29.4mm	-3563732.4638m	35.3mm

6. Adjusted Points in WGS84 (Geogr. Coordinates and Std.Dev.)

Point	Latitude	σ	Longitude	σ	Height	σ
HARB	S 25° 53' 13.05834"	0.0mm	E 27° 42' 26.06984"	0.0mm	1558.2684m	0.0mm
MBAR	S 0° 36' 05.27714"	44.8mm	E 30° 44' 16.34416"	124.9mm	1338.4651m	87.8mm
NKLG	N 0° 21' 14.07362"	61.3mm	E 9° 40' 19.64355"	191.2mm	32.3520m	109.0mm
RBAY	S 28° 47' 43.95956"	21.8mm	E 32° 04' 42.17320"	28.7mm	31.8141m	37.6mm
SIMO	S 34° 11' 16.57287"	27.8mm	E 18° 26' 22.45365"	30.5mm	39.7355m	44.4mm

7. Adjusted Points Error Ellipses

Point	Semimajor Axis	Semiminor Axis	Angle	95% confidence radius
HARB	0.0mm	0.0mm	90.0°	0.0mm
MBAR	124.9mm	44.8mm	-89.8°	249.1mm
NKLG	191.4mm	60.7mm	87.3°	380.1mm
RBAY	29.4mm	20.9mm	72.1°	63.3mm
SIMO	31.9mm	26.2mm	-59.0°	71.7mm

Appendix E: showing 3D Network Adjustment for Day of the year195 in 2008

Trimble

3D Network Adjustment for Day of the Year 195 in 2008

Project : M.TECH THESIS

User Name	UNIQUE	**Date & Time**	14:02:55 12/07/2010
Coordinate System	South Africa	**Zone**	Lo 17
Project Datum	Cape	**Geoid Model**	EGM96 (Global)
Coordinate Units	Meter		
Distance Units	Meter		
Height Units	Meter		
Angle Units	Degrees		

Network Adjustment in WGS84.	
Number of GPS Baselines	10
Number of Total Station Measurements	0
Number of Control Points in WGS84	1
Number of Adjusted Points	5
Confidence level	1 σ
Significance Level for Tau Test	1.00 %
Standard Error of Unit Weight	0.842
Number of Iterations	1
Refraction Coefficient	0.140

- Observations which were rejected by the statistical test are marked.

1. Baselines Input in WGS84 (Components and Std.Dev.)

Observation	ΔXm	σmm	ΔYm	σmm	ΔZm	σmm	Solution
HARB-MBAR	398293.9347	33.0	590117.6112	47.4	2701961.4087	16.4	Double Diff. / Float / Lc
HARB-NKLG	1202728.4568	40.4	-1598750.5063	57.3	2807614.1884	18.5	Double Diff. / Float / Lc
HARB-RBAY	-344891.8988	18.5	300433.1703	18.7	-285596.5205	10.3	Double Diff. / Float / Lc
HARB-SIMO	-74221.9928	18.1	-999730.5559	26.4	-795251.3150	11.3	Double Diff. / Float / Lc
NKLG-MBAR	-804434.5662	29.8	2188868.1462	42.4	-105652.7922	15.0	Double Diff. / Float / Lc
RBAY-MBAR	743185.8354	35.6	289684.4913	52.5	2987557.8996	18.1	Double Diff. / Float / Lc
RBAY-NKLG	1547620.4511	45.9	-1899183.7123	67.1	3093210.6802	22.4	Double Diff. / Float / Lc
SIMO-MBAR	472515.9743	34.9	1589848.2381	50.1	3497212.6679	18.6	Double Diff. / Float / Lc
SIMO-NKLG	1276950.5809	42.7	-599019.9557	61.9	3602865.4525	20.3	Double Diff. / Float / Lc
SIMO-RBAY	-270669.9081	20.0	1300163.7140	19.4	509654.7974	11.0	Double Diff. / Float / Lc

- Standard deviations of the static baselines have been multiplied with the factor 10.00.

2. WGS84 Control Points Input (Cart. Coordinates and Std.Dev.)

Point	X	σ	Y	σ	Z	σ
HARB	5084658.0099m	0.0mm	2670324.9794m	0.0mm	-2768481.0017m	0.0mm

3. Adjusted Baselines in WGS84 (Components and Std.Dev.)

Observation	ΔX	σ	ΔY	σ	ΔZ	σ

HARB-MBAR	398293.9462m	16.1mm	590117.6438m	22.8mm	2701961.3856m	8.3mm
HARB-NKLG	1202728.5172m	18.2mm	-1598750.5143m	25.7mm	2807614.1721m	8.9mm
HARB-RBAY	-344891.9047m	11.9mm	300433.1650m	13.1mm	-285596.5145m	6.6mm
HARB-SIMO	-74222.0039m	11.7mm	-999730.5549m	14.9mm	-795251.3063m	6.8mm
NKLG-MBAR	-804434.5710m	18.1mm	2188868.1581m	26.1mm	-105652.7866m	8.9mm
RBAY-MBAR	743185.8509m	16.5mm	289684.4788m	22.7mm	2987557.9001m	8.5mm
RBAY-NKLG	1547620.4219m	18.6mm	-1899183.6793m	25.8mm	3093210.6866m	9.2mm
SIMO-MBAR	472515.9501m	16.4mm	1589848.1987m	23.0mm	3497212.6919m	8.6mm
SIMO-NKLG	1276950.5211m	18.4mm	-599019.9594m	26.0mm	3602865.4784m	9.1mm
SIMO-RBAY	-270669.9007m	12.3mm	1300163.7199m	13.4mm	509654.7918m	6.8mm

4. Baseline Residuals (Residuals and Standardized Residuals)

Observation	Northing Res.	Stand. Res.	Easting Res.	Stand. Res.	Height Res.	Stand. Res.	Red.No.
HARB-MBAR	-9.7mm	-0.846	23.5mm	0.690	32.9mm	1.614	1.98
HARB-NKLG	7.1mm	0.504	-35.2mm	-0.833	51.9mm	2.007	2.09
HARB-RBAY	2.1mm	0.351	-1.9mm	-0.184	-9.5mm	-1.139	1.16
HARB-SIMO	3.7mm	0.622	6.0mm	0.363	-12.3mm	-1.256	1.44
NKLG-MBAR	5.7mm	0.495	12.7mm	0.496	-1.3mm	-0.095	1.44
RBAY-MBAR	3.8mm	0.317	-18.3mm	-0.485	6.9mm	0.271	2.11
RBAY-NKLG	1.2mm	0.070	42.8mm	0.837	-12.3mm	-0.379	2.32
SIMO-MBAR	4.2mm	0.394	-23.7mm	-0.643	-46.2mm	-1.981	2.04
SIMO-NKLG	-0.5mm	-0.037	24.5mm	0.533	-60.4mm	-2.032	2.18
SIMO-RBAY	-1.0mm	-0.169	1.8mm	0.159	10.8mm	1.116	1.24

5. Adjusted Points in WGS84 (Cart. Coordinates and Std.Dev.)

Point	X	σ	Y	σ	Z	σ
HARB	5084658.0099m	0.0mm	2670324.9794m	0.0mm	-2768481.0017m	0.0mm
MBAR	5482951.9561m	16.1mm	3260442.6232m	22.8mm	-66519.6161m	8.3mm
NKLG	6287386.5271m	18.2mm	1071574.4652m	25.7mm	39133.1704m	8.9mm
RBAY	4739766.1052m	11.9mm	2970758.1445m	13.1mm	-3054077.5162m	6.6mm
SIMO	5010436.0060m	11.7mm	1670594.4246m	14.9mm	-3563732.3080m	6.8mm

6. Adjusted Points in WGS84 (Geogr. Coordinates and Std.Dev.)

Point	Latitude	σ	Longitude	σ	Height	σ
HARB	S 25° 53' 13.05834"	0.0mm	E 27° 42' 26.06984"	0.0mm	1558.2684m	0.0mm
MBAR	S 0° 36' 05.28082"	8.2mm	E 30° 44' 16.34439"	23.5mm	1338.1294m	15.0mm
NKLG	N 0° 21' 14.07187"	8.9mm	E 9° 40' 19.64354"	26.5mm	32.2437m	17.0mm
RBAY	S 28° 47' 43.95938"	6.6mm	E 32° 04' 42.17329"	14.4mm	31.8403m	10.3mm
SIMO	S 34° 11' 16.57274"	6.8mm	E 18° 26' 22.45422"	15.7mm	39.4641m	10.6mm

7. Adjusted Points Error Ellipses

Point	Semimajor Axis	Semiminor Axis	Angle	95% confidence radius
HARB	0.0mm	0.0mm	0.0°	0.0mm
MBAR	23.5mm	8.2mm	-89.7°	46.9mm
NKLG	26.5mm	8.9mm	-89.8°	52.7mm
RBAY	14.4mm	6.5mm	-88.2°	29.1mm
SIMO	15.8mm	6.7mm	-86.1°	31.8mm

Appendix F: showing 3D Network Adjustment for Day of the year 01 in 2009

Trimble

3D Network Adjustment for Day of the Year 001 in 2009

Project : M.TECH THEIS

User Name	Tata Herbert	**Date & Time**	14:25:01 12/07/2010
Coordinate System	South Africa	**Zone**	Lo 17
Project Datum	Cape	**Geoid Model**	EGM96 (Global)
Coordinate Units	Meter		
Distance Units	Meter		
Height Units	Meter		
Angle Units	Degrees		

Network Adjustment in WGS84.	
Number of GPS Baselines	10
Number of Total Station Measurements	0
Number of Control Points in WGS84	1
Number of Adjusted Points	5
Confidence level	1 σ
Significance Level for Tau Test	1.00 %
Standard Error of Unit Weight	0.968
Number of Iterations	1
Refraction Coefficient	0.140

- Observations which were rejected by the statistical test are marked.

1. Baselines Input in WGS84 (Components and Std.Dev.)

Observation	ΔXm	σmm	ΔYm	σmm	ΔZm	σmm	Solution
HARB-MBAR	398293.6424	40.8	590117.4763	54.0	2701961.5496	18.0	Double Diff. / Float / Lc
HARB-NKLG	1202728.4222	53.2	-1598750.5799	79.8	2807614.3453	24.6	Double Diff. / Float / Lc
HARB-RBAY	-344891.8910	22.6	300433.1869	22.2	-285596.5478	12.1	Double Diff. / Float / Lc
HARB-SIMO	-74222.0105	28.6	-999730.5879	32.0	-795251.3123	15.7	Double Diff. / Float / Lc
NKLG-MBAR	-804434.8330	29.9	2188868.0941	41.1	-105652.7981	14.4	Double Diff. / Float / Lc
RBAY-MBAR	743185.5759	55.4	289684.3849	66.0	2987558.0568	23.6	Double Diff. / Float / Lc
RBAY-NKLG	1547620.4034	71.5	-1899183.8791	93.1	3093210.8278	29.4	Double Diff. / Float / Lc
SIMO-MBAR	472515.7542	42.6	1589848.0795	65.2	3497212.8046	19.6	Double Diff. / Float / Lc
SIMO-NKLG	1276950.5375	66.5	-599019.9010	93.7	3602865.5872	27.5	Double Diff. / Float / Lc
SIMO-RBAY	-270669.8792	32.4	1300163.7798	36.6	509654.7877	17.9	Double Diff. / Float / Lc

- Standard deviations of the static baselines have been multiplied with the factor 10.00.

2. WGS84 Control Points Input (Cart. Coordinates and Std.Dev.)

Point	X	σ	Y	σ	Z	σ
HARB	5084658.0198m	0.0mm	2670324.9589m	0.0mm	-2768481.0034m	0.0mm

3. Adjusted Baselines in WGS84 (Components and Std.Dev.)

Observation	ΔX	σ	ΔY	σ	ΔZ	σ
HARB-MBAR	398293.6719m	23.9mm	590117.5001m	31.2mm	2701961.5239m	10.9mm
HARB-NKLG	1202728.4869m	27.1mm	-1598750.5950m	37.2mm	2807614.3151m	12.4mm
HARB-RBAY	-344891.8977m	18.1mm	300433.1862m	18.7mm	-285596.5345m	9.4mm
HARB-SIMO	-74222.0324m	20.1mm	-999730.5971m	23.1mm	-795251.3024m	10.5mm
NKLG-MBAR	-804434.8149m	23.7mm	2188868.0951m	33.0mm	-105652.7912m	10.9mm
RBAY-MBAR	743185.5696m	25.5mm	289684.3139m	32.2mm	2987558.0584m	11.7mm
RBAY-NKLG	1547620.3846m	28.6mm	-1899183.7812m	37.9mm	3093210.8496m	13.0mm
SIMO-MBAR	472515.7043m	25.0mm	1589848.0972m	33.3mm	3497212.8263m	11.6mm
SIMO-NKLG	1276950.5192m	28.4mm	-599019.9979m	38.9mm	3602865.6175m	13.1mm
SIMO-RBAY	-270669.8653m	21.4mm	1300163.7833m	24.0mm	509654.7679m	11.1mm

4. Baseline Residuals (Residuals and Standardized Residuals)

Observation	Northing Res.	Stand. Res.	Easting Res.	Stand. Res.	Height Res.	Stand. Res.	Red.No.
HARB-MBAR	-6.9mm	-0.458	7.3mm	0.170	44.7mm	1.549	1.90
HARB-NKLG	-5.2mm	-0.259	-43.4mm	-0.616	58.4mm	1.486	2.18
HARB-RBAY	9.3mm	1.301	2.5mm	0.202	-11.4mm	-1.123	0.95
HARB-SIMO	-1.4mm	-0.163	2.0mm	0.088	-25.6mm	-1.448	1.41
NKLG-MBAR	13.4mm	1.131	-7.5mm	-0.328	11.7mm	0.886	1.03
RBAY-MBAR	-15.4mm	-0.892	-59.9mm	-0.973	-35.4mm	-0.892	2.21
RBAY-NKLG	32.2mm	1.332	95.5mm	1.094	16.5mm	0.295	2.41
SIMO-MBAR	3.8mm	0.255	38.8mm	0.757	-41.8mm	-1.146	1.96
SIMO-NKLG	0.5mm	0.021	-77.2mm	-0.908	-68.3mm	-1.300	2.37
SIMO-RBAY	-11.8mm	-1.283	-3.4mm	-0.121	21.2mm	0.929	1.58

5. Adjusted Points in WGS84 (Cart. Coordinates and Std.Dev.)

Point	X	σ	Y	σ	Z	σ
HARB	5084658.0198m	0.0mm	2670324.9589m	0.0mm	-2768481.0034m	0.0mm
MBAR	5482951.6917m	23.9mm	3260442.4590m	31.2mm	-66519.4795m	10.9mm
NKLG	6287386.5066m	27.1mm	1071574.3639m	37.2mm	39133.3117m	12.4mm
RBAY	4739766.1221m	18.1mm	2970758.1451m	18.7mm	-3054077.5379m	9.4mm
SIMO	5010435.9874m	20.1mm	1670594.3618m	23.1mm	-3563732.3058m	10.5mm

6. Adjusted Points in WGS84 (Geogr. Coordinates and Std.Dev.)

Point	Latitude	σ	Longitude	σ	Height	σ
HARB	S 25° 53' 13.05840"	0.0mm	E 27° 42' 26.06902"	0.0mm	1558.2684m	0.0mm
MBAR	S 0° 36' 05.27648"	10.9mm	E 30° 44' 16.34419"	32.7mm	1337.8167m	22.0mm
NKLG	N 0° 21' 14.07648"	12.5mm	E 9° 40' 19.64042"	38.4mm	32.2074m	25.3mm
RBAY	S 28° 47' 43.95977"	8.7mm	E 32° 04' 42.17298"	21.2mm	31.8635m	15.6mm
SIMO	S 34° 11' 16.57337"	10.0mm	E 18° 26' 22.45212"	24.6mm	39.4318m	18.5mm

7. Adjusted Points Error Ellipses

Point	Semimajor Axis	Semiminor Axis	Angle	95% confidence radius
HARB	0.0mm	0.0mm	90.0°	0.0mm
MBAR	32.7mm	10.9mm	89.7°	65.0mm
NKLG	38.4mm	12.5mm	89.5°	76.2mm
RBAY	21.2mm	8.7mm	-87.5°	42.5mm
SIMO	24.8mm	9.6mm	-82.6°	49.6mm

Appendix G: showing 3D Network Adjustment for Day of the year 02 in 2009

3D Network Adjustment for Day of the Year 002 in 2009

Project : M.TECH THESiS

User Name	Tata Herbert	**Date & Time**	20:08:08 12/07/2010
Coordinate System	South Africa	**Zone**	Lo 17
Project Datum	Cape	**Geoid Model**	EGM96 (Global)
Coordinate Units	Meter		
Distance Units	Meter		
Height Units	Meter		
Angle Units	Degrees		

Network Adjustment in WGS84.	
Number of GPS Baselines	10
Number of Total Station Measurements	0
Number of Control Points in WGS84	1
Number of Adjusted Points	5
Confidence level	1 σ
Significance Level for Tau Test	1.00 %
Standard Error of Unit Weight	1.278
Number of Iterations	1
Refraction Coefficient	0.140

- Observations which were rejected by the statistical test are marked.

1. Baselines Input in WGS84 (Components and Std.Dev.)

Observation	ΔXm	σmm	ΔYm	σmm	ΔZm	σmm	Solution
HARB-MBAR	398293.6740	37.6	590117.4848	53.9	2701961.4728	18.2	Double Diff. / Float / Lc
HARB-NKLG	1202728.4816	55.3	-1598750.4181	79.7	2807614.2656	23.2	Double Diff. / Float / Lc
HARB-RBAY	-344891.6427	27.0	300433.3057	29.1	-285596.6896	13.9	Double Diff. / Float / Lc
HARB-SIMO	-74221.9167	25.9	-999730.5636	27.5	-795251.3814	14.7	Double Diff. / Float / Lc
NKLG-MBAR	-804434.8803	31.0	2188868.0303	40.8	-105652.7996	14.9	Double Diff. / Float / Lc
RBAY-MBAR	743185.3870	49.6	289684.2125	70.9	2987558.1172	25.1	Double Diff. / Float / Lc
RBAY-NKLG	1547620.2314	77.9	-1899183.7857	105.8	3093210.8956	35.0	Double Diff. / Float / Lc
SIMO-MBAR	472515.6797	43.9	1589848.1415	68.9	3497212.7550	21.9	Double Diff. / Float / Lc
SIMO-NKLG	1276950.6163	89.4	-599019.8830	127.5	3602865.5029	40.5	Double Diff. / Float / Lc
SIMO-RBAY	-270669.7465	37.1	1300163.7982	44.5	509654.7485	20.9	Double Diff. / Float / Lc

- Standard deviations of the static baselines have been multiplied with the factor 10.00.

2. WGS84 Control Points Input (Cart. Coordinates and Std.Dev.)

Point	X	σ	Y	σ	Z	σ
HARB	5084658.0198m	0.0mm	2670324.9589m	0.0mm	-2768481.0034m	0.0mm

3. Adjusted Baselines in WGS84 (Components and Std.Dev.)

Observation	ΔX	σ	ΔY	σ	ΔZ	σ
HARB-MBAR	398293.6996m	30.7mm	590117.5219m	42.9mm	2701961.4378m	14.9mm
HARB-NKLG	1202728.5637m	37.2mm	-1598750.4923m	51.6mm	2807614.2327m	17.1mm
HARB-RBAY	-344891.6573m	26.8mm	300433.2933m	30.6mm	-285596.6712m	13.8mm
HARB-SIMO	-74221.9327m	26.2mm	-999730.5585m	29.5mm	-795251.3696m	14.3mm
NKLG-MBAR	-804434.8641m	32.5mm	2188868.0142m	44.6mm	-105652.7949m	15.2mm
RBAY-MBAR	743185.3569m	34.0mm	289684.2286m	46.2mm	2987558.1090m	16.9mm
RBAY-NKLG	1547620.2210m	40.1mm	-1899183.7856m	54.4mm	3093210.9040m	18.9mm
SIMO-MBAR	472515.6323m	33.3mm	1589848.0804m	45.9mm	3497212.8074m	16.7mm
SIMO-NKLG	1276950.4964m	39.9mm	-599019.9338m	54.5mm	3602865.6023m	19.1mm
SIMO-RBAY	-270669.7247m	30.5mm	1300163.8518m	35.6mm	509654.6984m	16.3mm

4. Baseline Residuals (Residuals and Standardized Residuals)

Observation	Northing Res.	Stand. Res.	Easting Res.	Stand. Res.	Height Res.	Stand. Res.	Red.No.
HARB-MBAR	-14.1mm	-0.727	21.0mm	0.381	51.2mm	1.480	1.81
HARB-NKLG	-12.9mm	-0.535	-103.9mm	-1.090	48.7mm	1.026	2.07
HARB-RBAY	8.4mm	0.639	-4.2mm	-0.180	-24.9mm	-1.388	1.15
HARB-SIMO	5.5mm	0.610	11.9mm	0.551	-15.7mm	-0.827	1.05
NKLG-MBAR	7.2mm	0.469	-21.8mm	-0.752	4.2mm	0.239	0.97
RBAY-MBAR	-15.7mm	-0.645	28.2mm	0.348	-13.6mm	-0.274	2.15
RBAY-NKLG	3.6mm	0.100	4.9mm	0.037	-11.8mm	-0.157	2.44
SIMO-MBAR	16.4mm	0.837	-32.1mm	-0.440	-86.2mm	-1.730	1.99
SIMO-NKLG	32.8mm	0.800	10.7mm	0.070	-160.2mm	-1.470	2.59
SIMO-RBAY	-25.8mm	-1.569	37.3mm	0.788	61.7mm	1.778	1.77

5. Adjusted Points in WGS84 (Cart. Coordinates and Std.Dev.)

Point	X	σ	Y	σ	Z	σ
HARB	5084658.0198m	0.0mm	2670324.9589m	0.0mm	-2768481.0034m	0.0mm
MBAR	5482951.7193m	30.7mm	3260442.4808m	42.9mm	-66519.5656m	14.9mm
NKLG	6287386.5835m	37.2mm	1071574.4666m	51.6mm	39133.2293m	17.1mm
RBAY	4739766.3624m	26.8mm	2970758.2522m	30.6mm	-3054077.6746m	13.8mm
SIMO	5010436.0871m	26.2mm	1670594.4004m	29.5mm	-3563732.3730m	14.3mm

6. Adjusted Points in WGS84 (Geogr. Coordinates and Std.Dev.)

Point	Latitude	σ	Longitude	σ	Height	σ
HARB	S 25° 53' 13.05840"	0.0mm	E 27° 42' 26.06902"	0.0mm	1558.2684m	0.0mm
MBAR	S 0° 36' 05.27927"	14.8mm	E 30° 44' 16.34434"	44.4mm	1337.8526m	28.5mm
NKLG	N 0° 21' 14.07378"	17.2mm	E 9° 40' 19.64328"	53.6mm	32.2999m	34.3mm
RBAY	S 28° 47' 43.95959"	13.9mm	E 32° 04' 42.17162"	33.3mm	32.1577m	23.3mm
SIMO	S 34° 11' 16.57322"	13.2mm	E 18° 26' 22.45232"	31.5mm	39.5579m	24.4mm

7. Adjusted Points Error Ellipses

Point	Semimajor Axis	Semiminor Axis	Angle	95% confidence radius
HARB	0.0mm	0.0mm	90.0°	0.0mm
MBAR	44.4mm	14.8mm	89.7°	88.3mm
NKLG	53.6mm	17.1mm	89.0°	106.4mm
RBAY	33.3mm	13.9mm	-89.8°	66.9mm
SIMO	31.7mm	12.7mm	-83.4°	63.6mm